



Estimating greenhouse gas emission via degassing and modeling temperature profiles in tropical reservoirs

Kvantifiering av växthusgasutsläpp vid
turbinpassage och modellering av
temperaturprofiler i tropiska vattenmagasin

Johan Wilson

REFERAT

Kvantifiering av växthusgasutsläpp vid turbinpassage och modellering av temperaturprofiler i tropiska vattenmagasin

Johan Wilson

Syftet med examensarbetet har varit att kvantifiera växthusgasutsläpp från vattenkraftsmagasin i tropiska regioner. Mer specifikt har fokus varit på emissioner i samband med att vattnet passerar kraftverkets turbin.

Vattenkraftsmagasin är en källa till utsläpp av växthusgaser till atmosfären och utgör 25 % av den totala arean av antropogena sötvattensystem, en andel som spås öka i framtiden. Planer finns att bygga ytterligare ca 3700 mellanstora till stora vattenkraftsverk, vilket kan leda till en fördubbling av den nuvarande globala energiproduktionen från vattenkraft. Merparten av dessa vattenkraftverk planeras i just tropiska regioner. Genom att förstå de processer som styr växthusgasutsläpp från vattenkraftsmagasin kan planering och design av nya vattenkraftverk vidareutvecklas för att minska utsläppen.

Detta arbete utformades för att undersöka växthusgasutsläppen från turbinerna av två magasin i Brasilien som en del av ett större projekt, Hydrocarb vilket har som syfte att studera växthusgasutsläpp från vattenkraftsmagasin i Brasilien. För att bestämma utsläppen när vattnet passerar turbinerna genomfördes en provtagningskampanj i magainet Chapeu D'Uvas. Vattenprover från hela vattenprofilen togs genom en ny typ av djupvattensprovtagare användes. Metankoncentration i vattenprofilen analyserades för att bestämma halten metan för varje segment av vattenpelaren vid dammens vattenintag, samt vid utloppet efter dammen. Resultatet visade att de djupa segmenten med låg syrekoncentration i vattenpelaren innehöll höga metankoncentrationer. Dock återfanns liknande höga koncentrationer även i vattnet direkt efter utloppet. Denna typ av provtagning var även planerad att genomföras vid vattenkraftsmagasinet Funil, men på grund av COVID-19 pandemin blev dessa kampanjer inställda. En modelleringstrategi utvecklades istället för att kunna bestämma metankoncentrationerna vid turbinernas vattenintag vid Funil, för att på så sätt kunna uppskatta utsläppen vid turbinen. Det första steget av modelleringen genomfördes i detta arbete, där kontinuerliga tidsserier av temperaturprofilen i magasinet bestämdes. De modellerade temperaturprofilerna visade temperaturer som stämde överens med observerade värden med ett fel (root mean square error) av 1,5 °C.

Slutsatsen av detta arbete är att metoden för att provta metankoncentration från olika djup av vattenprofilen var framgångsrik och kan användas för att undersöka metankoncentrationer vid de djup där vattenintaget sker hos vattenkraftsmagasin. Metanutsläppen från utflödet vid Chapeu D'Uvas var låga och står för 1,1 % av de totala utsläppen från vattenkraftsmagasinet. Resultatet från de modellerade temperaturprofilerna kan användas för att vidare bestämma syreförbrukningshastigheten och metanproduktionen i vattenkraftsmagasin.

Nyckelord: Metan, Växthusgaser, Vattenkraft

*Institutionen för geovetenskaper, Luft-, vatten- och landskapslära, Uppsala Universitet
Box 7032 Villavägen 16, SE-752 36 Uppsala
ISSN 1401-5765*

ABSTRACT

Estimating greenhouse gas emission via degassing and modeling temperature profiles in tropical reservoirs

The aim of this project was to quantify the greenhouse gas (GHG) emissions from the degassing process of hydroelectrical reservoirs in tropical regions.

Reservoirs represent 25 % of the total area of man-made freshwater systems and are a source of GHG emissions to the atmosphere. There are plans to construct an additional ca 3700 medium and large hydropower dams with the aim to double the current global energy production by hydropower. The majority of these are planned to be constructed in tropical regions. By understanding the processes controlling GHG emissions from these hydropower reservoirs, the design of new hydropower plants can be developed to minimize the emissions.

This project were designed to investigate GHG emissions from the turbines of two reservoirs in Brazil, as part of the larger "Hydrocarb" project that investigates the total emissions from a number of reservoirs in Brazil. To estimate the GHG emissions from the degassing process, a sampling campaign in the reservoir Chapeu D'Uvas was conducted in April 2020 .Water samples from the entire water column at the water inlet, and directly after the dam were taken by using a sampling technique that involved a newly developed deep-water sampler. The methane concentration was then analyzed for each depth of the water column and in the water directly after the outlet. The results showed that at the deep layers with low oxygen concentration in the water column contained high concentrations of methane. These high methane concentrations were also found in the water at the outlet.

This method was also planned to be used for the hydropower reservoir Funil, but due to the global COVID-19 pandemic the campaigns were canceled. A modeling approach was instead constructed with the aim to model the methane concentration at the intake of the water in Funil, and to estimate the degassing as the water passes the turbines. The first stage of this modeling approach was made within this study, where temperature profiles of the reservoir were modeled. The predicted profiles matched the observed temperatures profiles with a root mean square error of 1.5 °C. The study concluded that the method of collecting methane concentrations throughout the full water profile using the sampler were successful and can be used to examine methane concentration at the level of the water inlet in reservoirs. The methane emission from the outlet at Chapeu D'Uvas was estimated to be low contributing to 1.1 % of the total greenhouse gas emissions from the reservoir. For the modelling of methane concentration in water columns, the first part of the method to model daily temperature profiles that can be used to implement empirical models of oxygen demand and methane production in the model.

Keywords: Methan, Greenhouse gases, hydropower

*Department of Earth Sciences, Air, Water and Landscape Science, Uppsala University
Box 7032 Villavägen 16, SE-752 36 Uppsala
ISSN 1401-5765*

PREFACE

This master thesis is part of the master's Program in Environmental and Water Engineering at Uppsala University and the Swedish University of Agricultural Sciences. The thesis covers 30 Swedish academic credits and was conducted in collaboration with Hydrocarb team in Uppsala, Sweden and Juiz de Fora, Brazil. Supervisors were Sebastian Sobek, Associate Professor at the Department of Ecology and Genetics, Limnology, Uppsala University and examiner were Marcus Wallin at the Department of Earth Sciences at Uppsala University. I would like to give a big thanks to SIDA that founded the expenses covering the field work and to my supervisor Sebastian Sobek and to my subject reviewer Marcus Wallin. I have also had great help from Nathan Barros and Jose Paranaiba during the sampling camping in Brazil and of Simone Morras and Don Pierson for the modeling of the water temperature. Lastly, I would like to thank Yasmine Arriaga who been with me all the way of this project as my traveling partner while she conducted her own project in Brazil.

Johan Wilson
Uppsala 2021

POPULAR SCIENTIFIC SUMMARY

Measuring methane concentrations and modeling temperature profiles in tropical reservoirs to estimate methane emissions.

Johan Wilson

Svante Arrhenius, Nobel Laureate and Professor of Chemistry, published an article in 1896 in which he described how the carbon dioxide (CO₂) content in the atmosphere affects the Earth's average temperature. He then estimated that a doubling of the CO₂ content would increase the average temperature by 5.7 degrees. 105 years later, the UN Climate Panel estimated that a doubling would lead to an increase between 2.6 to 4.1 degrees. Arrhenius was the first to realize that the burning of fossil fuels would cause an increase in the Earth's temperature. Today we know that different greenhouse gases (GHG) have different radiative forcing, which is the gases ability to absorb energy from the sun. Different gases can only absorb energies of a certain wavelength but let through the rest. In order to be able to compare the climate effects of all the different atmospheric gases, the standardized term CO₂ equivalents is used as praxis. The difference between the concentration of methane (CH₄) in the atmosphere is 200 times smaller than of CO₂, but the global warming potential of CH₄ is 34 times greater than that of CO₂. Due to the strong global warming potential of methane, it has been estimated that CH₄ accounts for 75% of CO₂ equivalent GHG emissions from lakes and reservoirs in the world.

Reservoirs are a man-made aquatic system that affects the global water cycle. Hydropower plants were first considered a clean energy source with no emissions of GHG, but then research showed that hydropower reservoirs can be a potential source of GHG. These reservoirs cover an area of 3.4×10^5 km² and are about 25% of all the world's reservoirs. The need for more power in the world grows and it is planned to build around 3700 new medium and large hydropower dams are planned in the near future, which can double the current capacity. Hydropower is a renewable energy source and has a current estimated average for emissions of 18.5 g CO₂-eq / kWh, compared to coal-fired power plants emissions of 900 g CO₂-eq / kWh. By understanding the processes for GHG emissions from hydropower reserves, the design of new hydropower plants can be developed to minimize these emissions.

When reservoirs are created, land areas containing organic matter such as vegetation and soil are flooded. This organic material is then broken down by bacteria that consumes oxygen. As this process continues, there may be a lack of oxygen in the bottom water and reservoir sediment. In these oxygen-free zones, the organic material is then broken down into CH₄. Organic material is constantly added to the system in the form of the growth of algae and other plants, which can eventually become the main source of organic material in the reservoir continuing this process.

This work was designed to investigate GHG emissions from the turbines of two hydropower reservoirs in Brazil as part of a larger Hydrocarb project that has investigated the total emissions from a number of reservoirs in Brazil. The project had however to be cancelled due to the COVID-19 pandemic before the field work could be finished. Data from the tests of equipment and the methods from a drinking water reservoir were completed and have been analyzed to get an idea of the magnitude of the CH₄ concentration in the water column and the CH₄ concentration in the water after the outlet. The results show that at the oxygen-poor zones in the water column there were high concentrations of CH₄. These high CH₄ concentrations were also found in the water at the outflow. The measurements of the CH₄ concentrations for Chapeu D'Uvas showed that the highest concentration of 140 ± 13 mg m⁻³ was found at 25 meters. The concentration after the outlet was 120 ± 13 mg m⁻³. The release of CH₄ to the atmosphere were then estimated at 490 kg_{CO_{2e}} per day. When the project was interrupted before it could be completed, the project was reconstructed to try to model the CH₄ concentration at the intake of the water in Funil to estimate the degassing as the water passes the turbines. This method contained three steps, the first one being to model continuous temperature profiles of the reservoir, which later could be used to model oxygen consumption, and lastly the CH₄ production could be predicted from water temperature and oxygen concentration. For this project, the first phase of this setup was performed and the model predicted the seasonal change in stratification and mixing as well as predicted temperatures. The model was able to produce good estimations of daily water temperature profiles from a small number of historical profile data, and it can be used in the next step of the modeling approach.

WORDLIST

C	Carbon
CDU	Chapéu d'Uvas
CH ₄	Methane
CO ₂	Carbon dioxide
DOM	Dissolved Organic Matter
FNS	Furnas
FUN	Funil
IPCC	Intergovernmental Panel on Climate Change
<i>k</i>	Gas exchange coefficient (gas transfer velocity)
ppm	parts per million
UGGA	Ultra-portable GHG analyzer
GOTM	General Ocean Turbulence Model
ACPy	Auto calibration utility for GOTM

CONTENTS

Referat	I
Abstract	II
Preface	III
Popular scientific summary	IV
Wordlist	V
1 Introduction	1
1.1 Aims	2
1.1.1 Research questions	2
1.2 Layout of report	2
2 Background theory	2
2.1 Reservoirs in tropical regions	2
2.2 Gas dynamics in reservoirs	2
2.2.1 Surface diffusion and k-value	3
2.3 Degassing from turbine and downstream emissions	4
2.4 Model	4
2.4.1 GOTM	5
2.4.2 Organic carbon mineralization and CH ₄ formation in tropical reservoir sediment	5
3 Methods	5
3.1 Study sites	5
3.2 Study design	7
3.3 Measurement techniques	7
3.3.1 Deep-water sampler	7
3.3.2 Ultra-portable GHG analyzer	8
3.3.3 Measurement of deep-water gas concentrations	9
3.3.4 Diffusive surface measurements	9
3.3.5 Gas-Exchange Coefficient k	10
3.3.6 Degassing	11
3.4 Model	11
3.4.1 Water profile data and model calibration	11
3.4.2 Temperature model data collection	13
3.5 Future plans for modelling	14
3.5.1 Model approach	14
4 Results	15
4.1 Water profile of Chapeu D’Uvas	15
4.2 Vertical distribution of CH ₄ concentrations in the water profile	17
4.3 CH ₄ concentration after the dam	18
4.3.1 Gas-Exchange Coefficient	19
4.4 Modelled temperature profiles	21
5 Discussion	35
5.1 Measurements at Chapeu D’Uvas.	35
5.2 Modelled temperature profiles	36
5.3 Potential mitigation	37
6 Conclusion	38
Appendices	42

1 INTRODUCTION

Inland waters (rivers, lakes and reservoirs) play a vital role in the global carbon cycle as they are a significant sources of the greenhouse gases (GHG's) carbon dioxide (CO₂) and methane (CH₄) to the atmosphere. At the same time they bury more organic carbon (OC) in their sediments than the entire ocean (Cole et al. 2007, Battin et al. 2009, Tranvik et al. 2009, Aufdenkampe et al. 2011).

In the tropics, many new large hydropower dams are being built to meet the increasing energy demand of growing populations and economies. This is affecting GHG emissions and carbon cycling on a global scale. The global annual emission rates of CO₂ and CH₄, and consequently the global temperature increase is accelerating rapidly (Smith et al., 2015). Today hydroelectricity is the largest source of renewable electricity, but the contribution to climate change mitigation is not completely understood. The release of GHG from hydropower reservoirs varies depending on the location and the characteristics of the water chemistry, and in individual cases their emissions rates are comparable to thermal power plants (Scherer and Pfister, 2016). Not much is known about the magnitude of the emissions on a global scale but the carbon footprint of hydropower is far higher than what has previously been assumed (Hertwich, 2013). In the tropics, many new large hydropower dams are being built to meet the increasing energy demand of growing populations and economies, globally there are 3700 major dams being planned or are under construction (Zarfl et al., 2015).

Following flooding of landscapes to create any kind of reservoir, terrestrial plants die and no longer assimilate CO₂ by photosynthesis, resulting in the loss of a sink for atmospheric CO₂. In addition, decomposition of the organic carbon that was stored in plants and soils convert the carbon into CO₂ and CH₄, which are then released to the atmosphere. All of the reservoirs examined to date emit CO₂ and CH₄ to the atmosphere, but different landscapes contain different amounts of stored organic carbon in soil and vegetation (Torbert et al., 1997). Hence the potential for gas production and loss varies from site to site. For example, in the Boreal region of Canada, a worst-case scenario is flooded peatland because they contain a large store of organic carbon in peat, which can decompose and be returned to the atmosphere as GHG over a long period (Kelly et al., 1997).

The first studies of GHG fluxes from reservoirs focused on hydroelectric generation (Rudd et al., 1993, Kelly et al., 1997, Duchemin et al., 1995). It was, and still is, widely viewed as a carbon-free source of energy (Hoffert et al., 1998). This view likely originated because before 1994, there were no data available on CO₂ and CH₄ emissions from reservoirs, even though it was well known that oxygen depletion resulting from active decomposition of flooded organic matter was common in waters of newly constructed reservoirs (Rzóska, 1981). The first discussion of GHG emissions from reservoirs (Rudd et al. 1993) pointed out that GHG production per unit of power generated (e.g., in kWh) is not zero and should depend on the amount of organic carbon flooded to create the electricity. For example, reservoirs that flood large areas to produce few kWh, such as those built in areas with low topographical relief, would produce more GHG per kWh than reservoirs built in canyons where little area is flooded and large amounts of electricity are produced.

A study by Deemer et al. (2016) estimated that the global GHG emissions from reservoirs water surfaces account for 0.8(0.5-1.2) Pg CO₂ equivalents per year, with the majority of the emissions being caused by CH₄. It is consensus that CH₄ is the GHG of major concern, since the transformation of previously fixed atmospheric CO₂ to CH₄ in reservoirs implies a 34-fold amplification in global warming potential (IPCC 2013). In the study by Deemer et al. (2016) it is also stated that the uncertainty of the global estimate is very large. Another study conducted by Barros et al. (2011) estimates the global GHG emission from specifically hydropower reservoirs at of 48 Tg C as CO₂ yr⁻¹ and 3 Tg C as CH₄ yr⁻¹, corresponding to a total emission of 288 Tg CO₂-eq yr⁻¹, and given the increase in tropical hydropower, reservoir emissions are bound to increase in the future.

Looking at the overall studies done regarding GHG emissions from reservoirs there is a lack in understanding the magnitude and the regulations of GHG emissions and carbon burial. This in turn has a negative effect on the development of mitigation strategies to reduce GHG emissions from both planned and existing reservoirs. In the tropics this lack of knowledge is especially severe since this region has the highest emission rates stated by Barros et al. (2011) and it is also where most new hydropower are being planned to be built. There is a big market for building new hydropower reservoirs since the tropical regions like Africa and Latin America only use 8 and 25 % of their hydropower capacity (Kumar A, 2011).

One area where there is a lack in understanding the GHG emissions from reservoirs is through which pathways do the emissions occur. The main pathways of emissions are take is through diffusive fluxes from the surface of the water, ebullition in the form of bubbles of gas and the degassing at the turbine (the pathways are explained in

detail in section 2). Studies of the degassing process as the water passes the turbines has shown that there can be a large difference between the degassing rates, ranging from 3 - 1378 ton of $\text{CO}_{2\text{eqd}^{-1}}$ (dos Santos et al., 2017).

1.1 AIMS

This project will build on the hypothesis that *GHG emission at the turbine emission contributes significantly to total reservoir emission*. The project aimed to identify the magnitude of emission from the turbine of two reservoirs that vary in characteristics in terms of productivity (oligotrophic - eutrophic), size (9.5-35 km^2), and to relate that other emission pathways that were investigated in the Hydrocarb project. The research questions of the project are the following:

1.1.1 Research questions

- How big is the contribution of CH_4 and CO_2 emission from the degassing process during turbine passage for the total GHG emissions of tropical hydropower reservoir?
- Can the temperature profile of a tropical reservoir be modeled, in order to allow calculation of water column CH_4 concentration in the next step.

1.2 LAYOUT OF REPORT

This project was planned in beginning of 2020 and had the objective to measure the CH_4 and CO_2 emissions from the degassing process of one hydropower reservoirs and one drinking water reservoir. In the end of March the restrictions because of the pandemic of COVID-19 caused a shutdown of the university facilities, and the field work was stopped before the campaigns to the hydropower reservoirs could be performed. Data from one campaign to the drinking water reservoir Chapeu D'Uvas were able to be extracted. Upon returning, a modeling approach was developed to see if it was possible to model temperature profiles, in order to in the next step model oxygen consumption rate of the sediment together with the CH_4 production rates, and thus finally quantify CH_4 emissions from the degassing process. This report will be presented in a two-part structure, where the first part in each section relates to the results from the data collection at Chapeu D'Uvas, and the second part covers the modeling of water column temperature profiles.

2 BACKGROUND THEORY

2.1 RESERVOIRS IN TROPICAL REGIONS

Tropical reservoirs have the general characteristics of high temperatures of both the water and the sediment. These reservoirs often also have an anaerobic bottom layer. They generally also have a high supply of organic matter (OM) due to the high production of OM on land from terrestrial plants and in the water from phytoplankton, this does not necessarily give the reservoirs high OM concentration since the OM degradation at high temperatures is also very high (Winton et al., 2019). These conditions all contribute to the production of CH_4 and CO_2 . Not all tropical reservoirs are as productive, oligotrophic reservoirs as Chapeu D'Uvas has low productivity because of low nutrient content. In tropical regions a higher temperature results in a larger biological production of CH_4 in the reservoir since the temperature increase the activity of the microorganisms that break down the organic matter into CH_4 (Yvon-Durocher et al., 2014). The production of CH_4 is also occurring in tropical regions to a higher degree since the microbial processes that produce CH_4 is in need of an anaerobic environment. Seasonal water mixing usually is the result from changes in surface temperature, tropical reservoirs are not always affected by seasonal mixing since tropical regions can have a more stable yearly temperature. Reservoirs that do not have strong mixing of the water column for longer periods could lead to the buildup of the anaerobic layer that can develop over time and where CH_4 can be produced and then be emitted to the atmosphere. The CH_4 production is not constant throughout the reservoir's lifespan and emissions decline with the age of the reservoir but to what extent depends on the characteristics of the reservoir (Barros et al., 2011).

2.2 GAS DYNAMICS IN RESERVOIRS

Our world's rivers, streams and reservoirs account for a significant source of the atmospheric GHG (CO_2) and (CH_4) (Cole et al., 2007). These gases are mainly formed under different circumstances, the microbial degradation of organic matter in oxic environments mainly produces CO_2 . In anaerobic freshwater sediments the microbial degradation also produces CH_4 from breaking down organic matter. For the microbial degradation to occur organic matter is needed as a food source for the bacteria. The formation of a reservoir is done by damming a lake

or stream, this then floods the upstream area and organic matter is added to the reservoir through allochthonous sources which is organic matter formed in another place than where it is found and autochthonous sources which is organic matter formed in the place where it was found. The reservoirs can then begin to produce CH_4 when the carbon is transformed to CH_4 . CH_4 which has a 34 times higher warming potential than CO_2 in turn has a greater impact on global warming (Church et al., 2013). Not all CH_4 that is produced is directly released to the atmosphere it is estimated that up to 80% of the CH_4 that is produced in marine and freshwater environments is oxidized and never reaches the atmosphere. This happens through microbial oxidation. That makes microbial oxidation one of the largest CH_4 sinks on earth. (Reeburgh et al., 1993). The aerobic CH_4 -oxidizing bacteria (methanotrophs) use CH_4 as their only source of energy and the activity is driven by the availability of CH_4 . The CH_4 is then transformed to CO_2 by the methanotrophs.

The GHG that is produced can be released to the atmosphere from several different pathways from a reservoir see figure 1 for an illustration. The emission pathways are through diffusion from the water surface to the air called surface diffusion, through the release in form of gas bubbles called ebullition and from degassing when the gas is released through the turbine and through the evasion of the remaining excess of gases in the downstream out flowing water, generally called downstream emissions. The gases in the water is not evenly distributed throughout the entire water column. Reservoirs stratify thermally and accumulate high concentrations of CO_2 and CH_4 at depth when no mixing of the deeper layers occur (Kemenes et al., 2016). since the water intake of most hydropower plants is located in the deeper depth of the reservoir to provide pressurized water, this could have an effect on the total GHG emission from the hydropower reservoir.

The degassing process from dams take place when the drop of pressure from the bottom water near the inlet passes through the turbines and it release to an environment with atmospheric pressure, this result in a release of CH_4 and CO_2 to the atmosphere. The release of the gases does not occur at the same rate since the solubility of the gases in water differ, were CH_4 has roughly 65 times lower solubility in water than CO_2 . This results in the CH_4 being more affected by the pressure drop through the turbine since it has a lower solubility and therefore more prone to be released to the atmosphere (Abril et al., 2005).

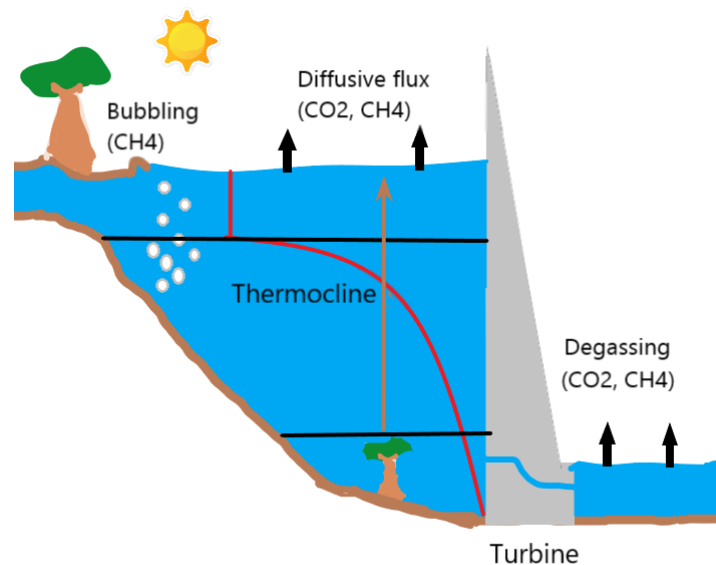


Figure 1. CH_4 (CH_4) and carbon dioxide (CO_2) emission pathways in a dammed reservoir. (Wilson 2020)

2.2.1 Surface diffusion and k-value

The diffusion of gases from the water surface is driven by the gas concentration gradient between the air and the water and by the gas transfer velocity k . For the diffusive fluxes of the gases the gas transfer value k is referring to the transfer speed of between the water surface and the atmosphere, the value is positively related to wind speed, rainfall and temperature (Gu erin et al., 2007). The value k is calculated by measuring the gas concentration over

time using a floating chamber. The flux between a water surface and air can then be calculated by using equation 1

$$F_{g,T} = \alpha k_{g,T} \delta P \quad (1)$$

$$\delta P = P_{w,g} - P_{a,g} \quad (2)$$

where $F_{g,T}$ is the flux at air–water interface for a given gas (g) at a given temperature (T), α is the solubility coefficient of the considered gas, $k_{g,T}$ is the gas transfer velocity (or piston velocity) for a specific gas at a given temperature, and P is the partial pressure gradient between water ($P_{w,g}$) and the overlying atmosphere ($P_{a,g}$).

2.3 DEGASSING FROM TURBINE AND DOWNSTREAM EMISSIONS

The degassing process of the different reservoirs is related to the outflow of water which differs depending on the size of the dam and the design of the outlet. How the water is released will have an impact on the degassing of the water. If the water is more turbulent a higher amount of CH_4 could potentially be released into the atmosphere. An example of the differences in the release can be seen in figure 2.



Figure 2. To the left its the outlet for Funil’s degassing process during high water levels and the picture to the right is the outlet for Chapeu D’Uv’as degassing process during high water levels (Wilson 2020).

Downstream dams the concentration of CH_4 is decreasing due to the diffusive emission to the atmosphere and through aerobic oxidation. When the dissolved CH_4 comes in contact with oxygen CH_4 oxidation accrues and is an important factor to take into account. The organisms transform the CH_4 into CO_2 and water.



The methanogenic oxidation happens in the reservoir as well when CH_4 rich water is transferred to surface water containing oxygen after the turbine. After the dam there is large amount of water with high CH_4 concentration, the CH_4 rich water from the hypolimnion that passes through the turbine suddenly comes in contact with oxygen and is re-oxygenated and a high CH_4 oxidation rate can occur (Guérin and Abril, 2007).

2.4 MODEL

The process of estimating GHG emissions relies on extensive sampling. By using these samples models for the processes can be developed leading to a more accessible tool for predicting the GHG of other reservoirs. There is one modelling tool for calculating a reservoirs carbon footprint, the tool G-res is an online tool used to predict the CO_2 and CH_4 emissions using empirical modelling based on measured reservoir fluxes with globally available environmental data. Predicting the emissions from future and present reservoirs is essential to be able to understand the impact reservoirs has on the global GHG emissions and an important tool for reservoir management. These tools are based on the current estimates and literature and is affected by the gaps and bias of current data

sets of the global reservoirs. To provide empirical data from regions with lesser data will help improve the estimations of current and future models. When building a model, the first step is to choose a suitable complexity of the model. A model with a lot of parameters will be good at predicting results for that specific environment but will be worse at predicting other systems. Models that are good at representing hydrodynamics of water such as vertical diffusion of oxygen and methane require a lot of input data to work. Lake 2.0 is a model that was developed by Stepanenko et al (2016) that can reproduce temperature, oxygen, CO₂ and CH₄ in the basin. The model includes a biogeochemical module and is tested on Kuivajärvi lake in Finland (Stepanenko et al., 2016). This model demanded input data that were not readily available for this study but could be a potential way to model the CH₄ in the future.

2.4.1 GOTM

GOTM is an acronym that stands for General Ocean Turbulence Model and is built as a one-dimensional water column model that is mainly used to study the hydrodynamics occurring vertically in the water column. The model is free for the public and is used and updated frequently. The structure of GOTM centers around a turbulence closure models for the parameterization of vertical turbulence fluxes of momentum, heat, dissolved organic matter and suspended particles (Burchard, 2002). The model can be coupled and added to other models or used as a standalone model for studying the dynamics of boundary layers in waters with the condition that the lateral gradient can be described. The GOTM simulates stratification processes and surface mixed-layer dynamics. The version of the GOTM model the GOTM-FABM were previously used in a study done by (Moras et al., 2019).

2.4.2 Organic carbon mineralization and CH₄ formation in tropical reservoir sediment

Sediments play an important role in the carbon cycle as they act as an active site for carbon storage and mineralization (Tranvik et al., 2009). For the sediments in freshwater ecosystems these processes are regulated by the availability of electron acceptors such as oxygen, nitrate, iron and sulfate it is also affected by the quantity of organic carbon and the mixing of the water column and temperature (Fenchel et al., 2012). Since the temperature effect the productivity of bacteria the OC mineralization rates significant increase with temperature. Factors as salinity, total nitrogen and chlorophyll are also important factors that control the OC mineralization for tropical reservoirs (Isidorova et al., 2019). The relationship of OC mineralization rates and temperature in lake sediments are described by a study that concluded that the Q₁₀ which expresses how OC mineralization respond to temperature (Van't Hoff, 1884). The Q₁₀ value for benthic and pelagic respiration for temperature range of 22-34 were calculated to 2.5. (Cardoso et al., 2014). The Q₁₀ of methanogenesis is typically high with a Q₁₀ of about 4 (Likens, 2009).

Strong relationships between temperature and CH₄ formation rates have been found in sediments of lakes and rivers (Wilkinson et al., 2015). Based on models predicting the effect of temperature on metabolic processes in sediments increasing temperature would lead to a higher organic carbon mineralization rates and as a result of that less carbon burial (Gudasz et al., 2010). Tropical systems have on average a higher temperature and higher mineralization in sediment CH₄ production (Yvon-Durocher et al., 2014). The methanogenesis relies on OM and the characteristics of the OM and the supply rate determine the production of CH₄. There is evidence that more CH₄ is produced from autochthonous OM in the form of aquatic plants and phytoplankton than from allochthonous OM from land plants and soils (West et al., 2012, Grasset et al., 2018). A study done by (Isidorova, 2019) measured the CH₄ formation rate in sediments of Chapéu D' Uvas (CDU), Curuá-Una (CUN) and Funil (FUN). The experiment were conducted through long term incubations of sediments and showed that the formation of CH₄ can be predicted from the sediment age and total nitrogen concentration.

3 METHODS

3.1 STUDY SITES

The reservoirs that is studied in this report are the two Brazilian reservoirs, *Chapéu d'Uvas*(CDU), a oligotroph drinking water reservoir and *Funil*(FUN), a eutrophic hydropower reservoir.

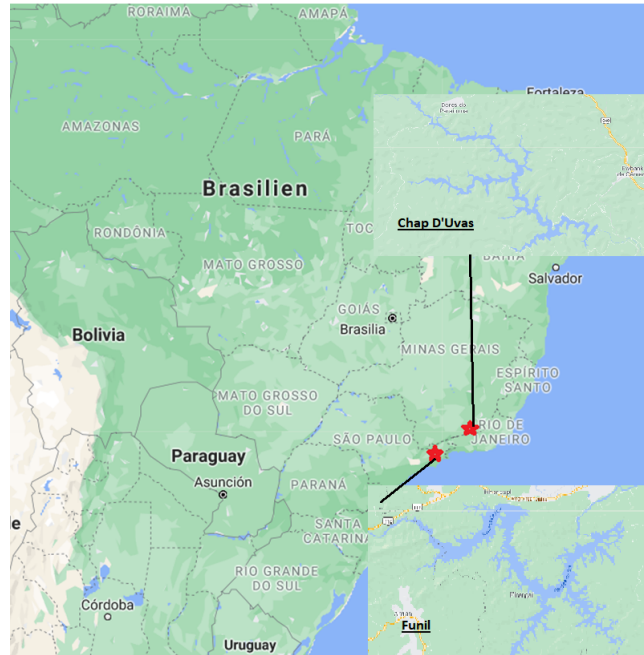


Figure 3. Map over the reservoirs locations in Brazil, maps from google earth. (Wilson, 2020)

The two reservoirs have different characteristics regarding size, age of the reservoir and trophic status. Chapéu d'Uvas has the coordinates S 21°33' W 43° 35' and its biome is Atlantic forest. It was first build for flood protection and later used as a drinking water reservoir since the oligotrophic water was clear and it started its first production for water supply 1994 The reservoir surface area is 9.5 km² and the catchment area of the reservoir is 310 km². The mean total phosphorus is 12 μg L⁻¹ and the mean total nitrogen is 452 μg L⁻¹, see table1. *Funil* has the coordinates S 22°31' W 44° 34' and its biome is Atlantic rain forest. The hydropower reservoir was constructed in 1969. The installed generating capacity of the plant is 180 MW with the hydraulic design head of 39 meter. The reservoir surface area is 35 km² and the catchment area of the reservoir is 13518 km². The residence time for the reservoir is 0.09 years. The mean total phosphorus is 34 μg L⁻¹ and the mean total nitrogen is 1279 μg L⁻¹. The water chemistry measurements (phosphorous, nitrogen) in the reservoirs CDU and FNS originate from a sampling campaigns(Linkhorst, 2019). The total annual precipitation for both reservoirs is 1597 mm and the value come from the same meteorological station.

Table 1. Characteristics of the reservoirs Chapéu D'Uvas and Funil

	Chapéu d'Uvas	Funil
Location	S 21°33' W 43° 35'	S 22°31' W 44° 34'
Reservoir use	Water supply	Hydro electricy
Area (km ²)	9.5	35
Catchment area (km ²)	310	13518
Residence time (yr)	n.d	0,09
Mean total phosphorus (μgL ⁻¹)	12	34
Mean total nitrogen (μgL ⁻¹)	452	1278
Annual precipitation (mm)	1597	1597

The water quality data come from an earlier study done by (Paranaíba et al., 2018) which examined the spatial variability and the drivers for diffusive fluxes measurements in Chapéu D'Uvas. The parameters that where measured were water temperature, pH, conductivity, oxygen concentration, chlorophyll and turbidity. The measurements were done by using a multi parameter probe (YSI 6600 V2) which logged every 30 seconds.

3.2 STUDY DESIGN

The first part of the study was to define the water profile by measuring, dissolved oxygen, temperature, turbidity, conductivity and pH. This was done using the YSI 6600 sond. Next water samples were taken next to the inlet of the dam with four replicas at every 5 meters. Water samples were also taken after the dam with four replicas at 1 meter depth. Air samples 1 meter above the water surface was also collected. These samples were analyzed using a gas analyzer to obtain CH₄ and CO₂ concentrations. With the concentrations of the inlet and the concentration at the outlet after the turbine and knowing the discharge an estimate of the GHG emissions from the degassing process at the turbine can be calculated.

3.3 MEASUREMENT TECHNIQUES

For this report the only measurements that were able to be collected were from Chapêu d'Uvas, the sampling took place in two locations. One for the samples in the reservoir, right in front of the water inlet called location A (-21.58353, -43.52827) and one location right after the water outlet called location B (-21.58521, -43.52632). The reservoir and the location is shown in figure 4.

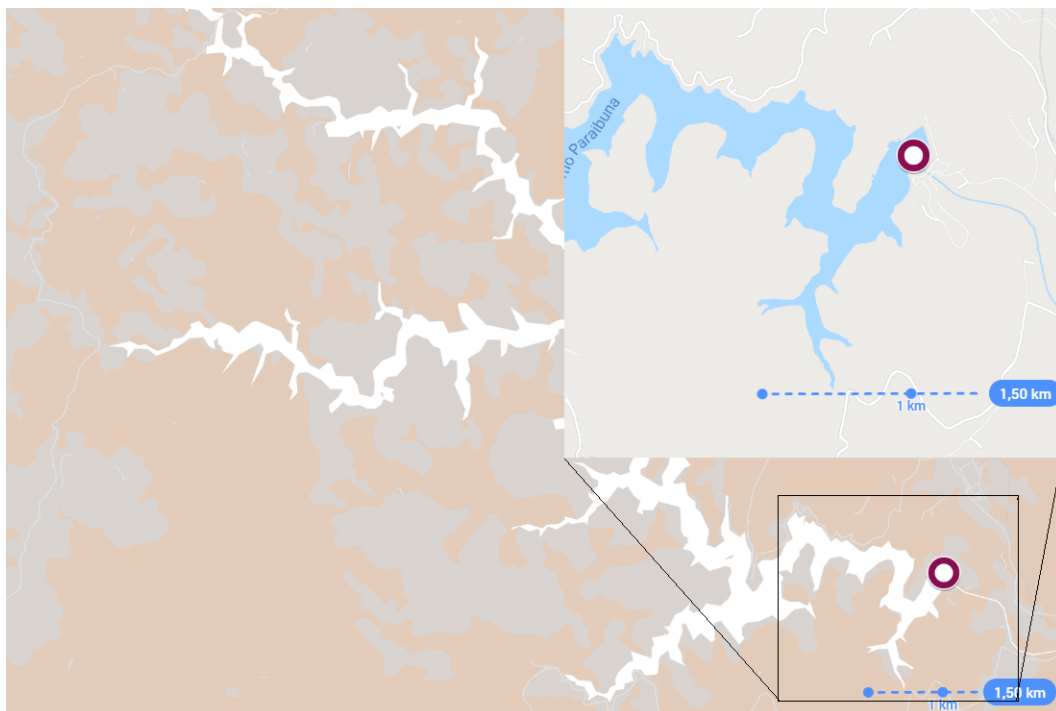


Figure 4. Map over Chapêu D'Uvas with the sampling locations marked with a red dot. Map from google earth (Wilson, 2020)

3.3.1 Deep-water sampler

For the water sampling in deep-water a special sampler was created by the Hydrocarb team which is a joint research project of Limnology program at Uppsala University (UU) and the Aquatic Ecology Laboratory at the Federal University of Juiz de Fora (UFJF, Brazil). It is constructed by assembling four 60 ml syringes that are mounted on a horizontal metal cross where the top part of the syringes are fixed in place. Vertical from the middle of the steel cross there is a steel bar which holds the cylindrical syringes in place and can be lowered down making the syringes fill up. The syringes are being kept in place as they are lowered and only when sending down a weight along the rope does the syringes detach and begin to be drawn down by the weight attached at the bottom. At the end of the syringes there are three-way valves which in the beginning are open, the valve is connected to the fixed metal cross with a wire which makes it turn as the syringe gets longer and fills up. When the syringes are fully extended the valve close and seal the syringe. A picture of the deep-water sampler (DWS) being tested in an aquarium can be seen in figure 5.



Figure 5. Deep-water sampler being tested in aquarium

The DWS was tested before the first field campaign to see if water was leaking into the syringe on the decent. This test was performed by lowering the DWS without sending a weight called (messenger-weight) down with the valve open and after 1 minute taking the sampler back up. This test showed that there were no water leaking into the syringe without the messenger being sent down. After this test affirmed that the DWS only collects water from the desired depth the sampler was tested by releasing the messenger. The DWS was then pulled up and the syringes was containing 20 ml of water. The 4 water samples were treated separately. The water was transferred to a 60 ml syringe containing 10 ml ambient air, the syringe was then shaken vigorously for 2 minutes for the air to reach equilibrium. Then the gas phase was transferred to a 10 ml syringe which is injected to the ultra-portable GHG analyzer (UGGA). So, for each depth 4 samples were collected and analyzed to result in 4 data points. The discrete samples collected after the dam were collected using the DWS and contained three air samples 1 m above the water surface and four samples of surface water.

3.3.2 Ultra-portable GHG analyzer

For the analyzing of CH_4 and CO_2 concentrations in the water samples from the reservoirs, the ultra-portable GHG analyzer from ABB was used for surface water samples and deep-water samples. The UGGA registers values at a 1 Hz (one measurement per second). For the discrete samples from the water samples the UGGA was equipped with a tube that had a three-way valve which made it possible to allow for two gas flows to be interchangeably applied (Paranaíba et al., 2018). The UGGA could be connected to a custom-made tube containing a soda lime cartridge that absorbed any CO_2 from the atmosphere. For the analyses the baseline for CO_2 was 0 ± 0.1 ppm and

for CH₄ it was 1.8 ± 0.1 ppm. The three-way valve allowed for the discrete samples to be mounted to the third entry valve which could then be turned to block the baseline gas flow. With the baseline being closed off only gas from the syringe flowed to the UGGA. The flow into the inlet port was driven by the internal pump in the UGGA. This made so that when the sample syringe was connected to the three-way valve and the system were open to the syringe and the UGGA the gas could be sucked into the UGGA without any external force. After the injection of a sample the flow was turned back into the baseline air flow. The time of the injection was noted down, and the peak concentration was recorded by the UGGA and the area under the peaks were calculated using a R script. The script can be found in the appendix 6.

3.3.3 Measurement of deep-water gas concentrations

The measurements of the CH₄ concentrations for the quantification of the GHG emission from the degassing by the turbine was done by sampling the horizontal water column. The water column was first measured by using a YSI 6600 multi-variable probe which made continuously measurements of water quality parameters, the sonde was lowered each meter and was kept at that depth for 1 minute. The concentration of CO₂ and CH₄ is calculated by analysing water samples as stated in previous chapters. After the water profile was measured, 8 sampling depth were decided. The gas phase from the samples was then analyzed in the UGGA as stated in previous chapters. The area that the peak produces corresponds to the concentration of the gases in the water, and the value was corrected with a calibration of the area in ppm to mol (the correction is displayed in the R script, in appendix). A excel sheet was prepared for the conversion from mol to mg m³ by knowing the air temperature and the pressure for the time of the sampling and the time of the injection into the UGGA, developed by Jose Paranaiba at Federal University of Juiz de Fora (the equations can be found in appendix).

3.3.4 Diffusive surface measurements

The surface diffusion is the gas flux from the water surface to the air that is driven by the gradient in gas partial pressure. The surface diffusion of CO₂ and CH₄ was measured at one location for Chapeu D'Uvas. The fluxes were measured using a floating chamber connected in a closed loop system to the UGGA see figure 6. The floating chamber was cylindrical in shape, the volume of the chamber was 17 L and 0,007 m² surface area. The bottom of the chamber was composed of a polyethylene foam ring that made the walls of the chamber extending 5 centimeters into the water column. The surface diffusion rate was calculated from the linear change in CO₂ and CH₄ partial pressure through the time inside the chamber. The concentration from the discreet surface samples was measured using the head space technique. Surface water was collected in three, 60 ml gas-tight plastic syringes and filled with 20 ml of surface water and 10 ml of ambient air. The syringe was shaken for 2 minutes to achieve gas equilibrium between the gas and the water phase. The 10 ml head space was transferred to a second syringe, and then injected in the UGGA.

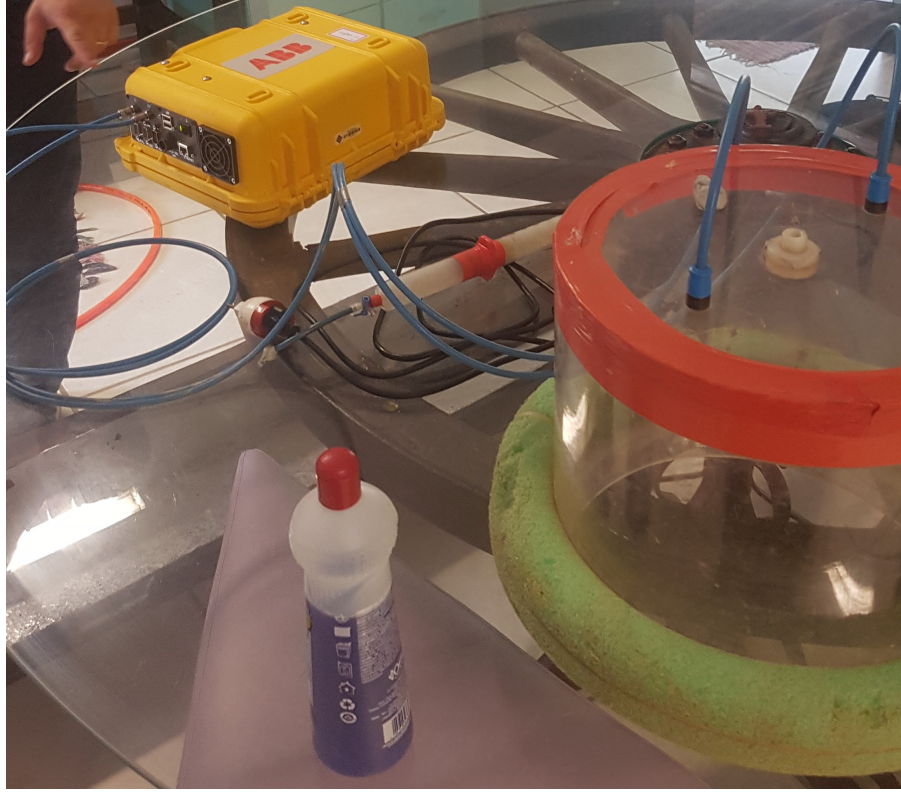


Figure 6. Floating chamber connected to the UGGA.

3.3.5 Gas-Exchange Coefficient k

For the calculation of the k -value floating chamber measurements and discrete measurements were performed at the site. The floating chamber was deployed 20 meters from the inlet of the drinking water. The floating chamber was deployed three times and was drifting with the boat during the measurement to avoid creating artificial turbulence. The floating chamber was connected with a tube to the UGGA forming a closed loop system to quantify the changes for CO_2 and CH_4 concentration inside the chamber. Each deployment lasted 3 minutes. The UGGA allowed for real time display of the concentration inside the chamber, making it possible to control that the deployment was not aborted too early. It also minimized the time that the chamber was needed to be deployed and thereby to limit the temperature change inside the chamber. The chamber deployment was discarded if a linear regression between the concentration and the time resulted in a R^2 value below 0.9 indicating a nonlinear behavior that may be related to gas bubbles enriched in CH_4 adding to the concentration of the chamber. The geographical position of the sampling site was noted using a handheld GPS device. Diffusive gas flux depends the concentration gradient between the air and water surface and the gas exchange velocity k for a specific gas at a specific temperature. The concentration gradient is expressed as the difference between the actual concentration of gas in the water and the concentration that water would have had if it were in equilibrium with the atmosphere (Cole and Caraco, 1998). This can be given by the equation,

$$F_{g,T} = k(P_{gas}K_h - C_{eq}) \quad (4)$$

where C_{eq} is the concentration of gas the water would have at equilibrium with the overlaying atmosphere, $P_{gas} \times K_h$ is the concentration of the water, where K_h is Henry's constant for the gas at a given temperature and salinity and P_{gas} is the partial pressure of the gas in the surface water. The k -value were derived from measurements of gas flux from the floating chamber measurements and the partial pressure of CO_2 and CH_4 and given the notation k_{FC}

$$k_{FC} = \frac{(P_{gas}K_h - C_{eq})}{F_{g,T}} \quad (5)$$

3.3.6 Degassing

The degassing of CO₂ and CH₄ from water passing the dam was derived from following equation.

$$C_{deg} = Q(C_{up} - C_{down}) \quad (6)$$

were Q is the discharge and C_{up}, C_{down} is the upstream gas concentrations measured at the water intake depth. Gas concentrations upstream and downstream of the dam were obtained by measuring the CO₂ and CH₄ concentration in a vertical water profile upstream the dam. The sampling directly downstream the outlet of the reservoirs was done by first using the deep-water sampler and lowering it as close to the surface as possible and sampling the air concentration of CH₄ and CO₂ to correct for the amount of concentration of the gases in the headspace air. Then surface water directly after the turbine outflow was sampled. Sampling locations is playing a big role and for each location specific places were chosen to have a safe place to sample from. The measurements at Chapeu D'Uvas water outlet were taken at the location shown in figure 7.



Figure 7. The outlet of Chapeu D'Uvas, the picture to the left shows a outflow of surface water from the spillway that is activated when the reservoir is at max capacity. The right picture shows the outflow from the water intake at 35 meters depth

3.4 MODEL

The approach to model for this study was set into three stages, the first was to model daily temperature profiles based on historical water profiles from Funil. Only this first step of the model strategy was done in this report. The model is adopted to reconstruct daily profiles of water temperature from data sets that span a short period of time or are incomplete. The model was used for the lake Erken in Sweden and the model is validated for the 70-year measurements that is recorded from Erken (Moras et al., 2019). Feeding the model is meteorological data and historical water temperature profiles. It uses seven climatic parameters as forcing data that include, wind, air pressure, air temperature, precipitation, humidity, cloud cover and short-wave radiation.

3.4.1 Water profile data and model calibration

The model used in this study to produce daily temperature profiles was the GOTM based model. What the model needs to operate is meteorological data and water layer data. The model parameters need to be calibrated to fit the observed data of Funil. The data is 8 parameters that include, wind speed, cloud coverage, shortwave radiation, precipitation, air temperature. The calibration of the model was done by using scaling factors for some of the parameters. The model parameters that are calibrated with scaling factor's are the heat flux, wind, short-wave radiation, e-folding depth that is the depth of the visible fraction of incoming radiation and the minimum turbulent kinetic energy.

The water level for this study is set to a fixed mean based on the annual mean of the water level of Funil. The ice cover module of the model was disabled for this study. For the model to work it has to have a starting point

of a measured water column. The starting date of the model is the first measured profile that was measured in 2017-10-01. The model simulated data points for the water column for each day from the start date to 2020. A commonly used method in modeling is the use of a split calibration and validation approach in which half of the data set is used to calibrate the parameters and the other half is used to validate the model. But for this study the goal is to simulate within the calibration period the whole data set is used to calibrate the model parameters in order to get the best fitted model. For this study the model was calibrated manually as well as using the ACPy (Auto Calibration Python) program, which eliminates the need for manual calibration and accelerates the process of finding good parameter values. The ACPy also allows for a more extensive testing and evaluation of the calibration for the model which in turn results in a more accurate result. A set of model parameters is calibrated and adjusted within the boundaries for realistic maximum and minimum values. This restriction is done to reduce the risk of pushing the parameter values to far in one direction. The calibration aims to reduce the difference between the simulated and the measured water temperature. The model parameters are non-dimensional scaling factors that adjust the heat flux, wind and short-wave radiation. It also adjusts the minimum turbulent kinetic energy and the light extinction depth which is the depth for the visible fraction of the incoming radiation. These are the parameters which influence the vertical distribution of light and temperature throughout the water column (Moras et al., 2019) In order to get stable initial values the first year is set to be the spin up year simply by using a copy of the data from the first year so that the first year is both used as a spin up year and then reused in the calibration. The ACPy is using a differential evaluation algorithm that calculate a log-likelihood function which compares the modelled water temperature to the observed temperature. The likelihood is defined by the equation

$$A = - \sum_i \frac{(x_{obs,i} - x_{mod,i})^2}{var_x} \quad (7)$$

where $x_{obs,i}$ is the observed temperature, $x_{mod,i}$ is the modeled temperature, and var_x is the variance between the modelled and the observed temperature. After the calibration the model fit can be evaluated based on estimation of bias, mean absolute error (MAE) and the root mean squared error (RMSE).

Calibrating the model using the scaling factor $s_{heatflux}$ changes how much the heat fluxes at the surface effect the model. Lower values result in higher water temperatures and a higher value lower temperature. The short-wave radiation scaling factor s_{SWR} effects how much the values from the measured SWR is effected. SWR determines how much the radiation from the sun heats the water and affects the temperature of the whole profile. With a low scaling factor, the SWR is reduced and lowers the temperature in the profile and a high scaling factor it increases the temperature. The scaling factor for the wind s_{wind} affects how much the wind speed affects the model, and lower values result in less mixing of the water column and higher values in higher mixing. The scaling factor for e-folding depth of visible shortwave radiation $s_{e-folding}$ affects how far down the visible radiation reaches in the profile. A higher value results in less stratification in the upper layers and higher temperatures further down and a lower values gives more stratification higher up in the column and lower temperatures in the deeper layers. The minimum turbulent kinetic energy scaling factor $s_{minkineticenergy}$ affects how low the minimum turbulence in the water column can be. With lower values the mixing in the column is less and with higher values the mixing is higher.

The air temperatures can change fast in tropical climates depending on when on the day the temperature is measured. To try to account for this a scaling factor for the air temperature was included in a later stage of the calibration. The scaling factor adjusts the air temperature and for low values the temperature in the surface of the profile is lower and for higher it becomes higher.



Figure 8. Location of the water profile sampling points, map from Google earth (Wilson, 2020)

60 temperature profiles were selected to be used as input data for the model. Data was used from sites that were more than 20 m deep, in order to capture thermocline depths that can be expected in the dam basin with its 62 m see figure 8 taken from Earth (2020).

The model was calibrated using the ACPy calibration with 10.000 iterations. More than one calibration using different boundary conditions were performed to try to find the best fit of the model. The model was then calibrated manually to get the best model fit in the deeper levels of the reservoir. The statistical analysis was done using R studio and the model fit was tested based on the root mean square error (RMSE). The model fit was tested for the entire profile 0-60 meter and for the lower parts 20-60 meters. For the first ACPy calibrations the scaling factors included the same as the manual calibration that were, Heat-flux, SWR, Wind, Min turbulent kinetic energy and e-folding depth. Another calibration of the model was performed with the added air temperature scaling factor. For this calibration the boundaries were also increased for the e folding depth and decreased for the SWR factor.

Table 2. Parameter sets from the ACPy, APCy with added temperature scaling factor and the manual calibration for entire calibration period between 2017 and 2020

Model parameter	Manual	ACPy	ACPy air t	Parameter range
Heat-flux factor	0.769	0.828	0.938	0.5-1.5 ; 0.5-1.5
Shortwave radiation factor	0.962	0.500	0.802	0.5-1.5 ; 0.8-1.2
Wind factor	1.424	1.499	1.499	0.5-1.5 ; 0.5-1.5
Min turbulent kinetic energy	8.417×10^{-6}	2.664×10^{-6}	9.160×10^{-6}	1×10^{-7} - 1×10^{-4}
e-folding depth	1.910	1.002	9.999	1.0-2.0 ; 1.0-10
air temp factor	-	-	0.940	0.8-1.0

3.4.2 Temperature model data collection

The water profile data that is fed into the model comes from field measurements of the water profiles that were collected during 2014-2019 by the Hydrocarb team in Brazil. The meteorological data is retrieved from the meteorology station 20 km from Funil in Resende and was provided by INMET (Insituto Nacial de Meteorologia, Brazil). Wind, air pressure, air temperature, humidity, cloud cover data and precipitation were daily values. The short-wave radiation were hourly values of short-wave radiation in $W m^{-2}$. Missing data points were in the

first stage set to 0 so that the model worked. In a later stage these values were linearly interpolated from the adjacent values. The calculation of the hypsograph for Funil were done by using bathymetry data collected by Annika Linkhorst in 2015. The data were collected using an echosounder (Linkhorst, 2019). The bathymetry and hydrograph data and can be found in the appendix.

Table 3. Data points for the different data files used for the temperature profile model.

File	Data points
Precipitation	2275
Meteorology data	5163
short-wave radiation	51260
Waterprofiles	60

3.5 FUTURE PLANS FOR MODELLING

The further development of the modeling approach includes the calculation of oxygen consumption rate from the sedimentation from the modeled bottom water temperature. This would be done using the regression described in section 4.3 and based on the regression by (Cardoso et al., 2014). The third step was to let the model run in daily time steps until the bottom layer above the sediment start to become anoxic. By then the CH₄ production would be implemented into the model. The model would let CH₄ diffuse into the bottom water according to the CH₄ production measured by (Isidorova et al., 2019). The model would be set to 60 meters depth and with layers of 1 meter and run with the daily time steps and the anoxia and the CH₄ concentration would move upwards in the water column in 1 meter steps. So, when the lowest layer would become anoxic the oxygen consumption would continue to the next water layer. Only the first step of the model strategy where done in this report.

3.5.1 Model approach

From the available data a simpler model strategy was developed. By using water column profiles of temperature, the characteristics of mixing type and approximate length of stratification for the reservoir could be predicted. Then during stratification and using the mean stratification depth the oxygen consumption rate of the sediment can be calculated from the bottom water temperature. Once the layer is anoxic the model can let CH₄ diffuse into the bottom water according to the CH₄ production further explained in section 4.3. The model would run with daily time steps and the anoxia and the CH₄ concentration progress upwards in the water column in a stepwise way. A sketch of the model is shown in figure 9.

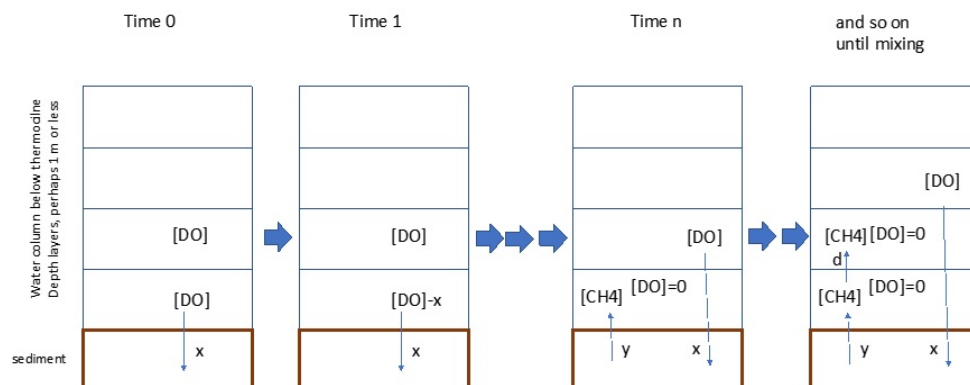


Figure 9. Sketch of model approach (Sobek,2020)

x is the flux of dissolved oxygen i.e the sediments O₂ consumption rate. DO indicates the dissolved oxygen concentration. y is the flux of dissolved CH₄ i.e the sediments CH₄ production rate and d is the diffusivity. The first step of the model is to produce continuous water temperature profiles that is needed as a input to calculate the oxygen demand of the sediment. To predict the temperature profiles the GOTM-FABM setup was used.

4 RESULTS

4.1 WATER PROFILE OF CHAPEU D'UVAS

The temperature, conductivity, dissolved oxygen (%), dissolved oxygen (mg l^{-1}), pH and turbidity were measured down to 33 meters depth, lower than that the measurements did not stabilize enough to record a stable value. The water quality values are shown in table 4. The water temperature and the dissolved oxygen are the two parameters which are of most interest. From the temperature data there can be seen a trend of lower temperature with descendent depth with the highest temperature at $29\text{ }^{\circ}\text{C}$ at the surface and the lowest temperature at $22\text{ }^{\circ}\text{C}$ at the bottom. The dissolved oxygen is also decreasing with depth were the concentration at the surface is $8.37\text{ (mg l}^{-1}\text{)}$ and with the lowest concentration close to the bottom where it was $0.46\text{ (mg l}^{-1}\text{)}$. The temperature and oxygen profile are plotted to visualize the trend. Analyzing the temperature profile and looking at stratification that has a difference of more than 1°C per 1m depth, the temperature is clearly showing stratification at the surface layers. The upmost temperature is (29°C). The dissolved oxygen (DO) is supersaturated for the upmost layer and indicates a temporary stratification that can occur during a warm and sunny day with high phytoplankton productivity that produce DO. The DO is low for the layers below 5 m depth and the water must have been isolated from the atmosphere during a extended period. Below 20 meters depth the water is anoxic or close to anoxic. No clear thermocline on the deeper depths can be observed from the collected data. From the oxygen data a decreasing trend can be clearly displayed. This is shown in figure 10 and 11.

Table 4. Chapeu D'Uvas water quality data for depth 0-33 mm. Parameters for each depth are Temperature ($^{\circ}\text{C}$), Conductivity (μScm^{-1}), Dissolved oxygen (%), Dissolved oxygen mg l^{-1}), pH and Turbidity (FNU). The measurements are discrete data from a YSI sond.

Depth(m)	Temp($^{\circ}\text{C}$)	Cond (μScm^{-1})	DO(%)	DO(mg l^{-1})	pH	Turb(FNU)
0	25.32	32	113.2	8.46	7.26	7.7
1	29.19	29	101.7	8.37	6.98	7.8
2	25.07	29	95.8	7.9	6.86	7.8
3	24.6	29	76.1	6.25	6.7	8.1
4	24.44	29	50.4	4.87	6.67	8.2
5	24.15	30	30.6	2.57	6.49	8.7
6	23.77	31	25.8	2.02	6.35	8.5
7	23.54	31	15.5	1.29	6.22	9.3
8	23.39	31	15.2	1.25	6.23	9.1
9	23.22	31	16.8	1.44	6.21	9.2
10	23.9	31	17.9	1.50	6.17	9.2
11	22.99	31	19.6	1.69	6.14	9.1
12	22.92	30	19.6	1.68	6.11	9.4
13	22.86	30	21.3	1.83	6.11	9.1
14	22.75	31	20.1	1.79	6.08	9.1
15	22.65	31	19.5	1.65	6.03	9.4
16	22.55	30	21.2	1.84	5.98	9.4
17	22.49	30	21.3	1.89	5.96	9.2
20	22.32	31	9.5	0.85	5.90	9.5
23	22.26	24	5.8	0.51	5.85	16.1
26	22.33	24	5.7	0.50	5.84	44.9
27	22.33	31	5.5	0.46	5.88	24.7
30	22.23	31	5.7	0.50	5.91	22.0
33	22.24	31	5.9	0.51	5.92	21.4

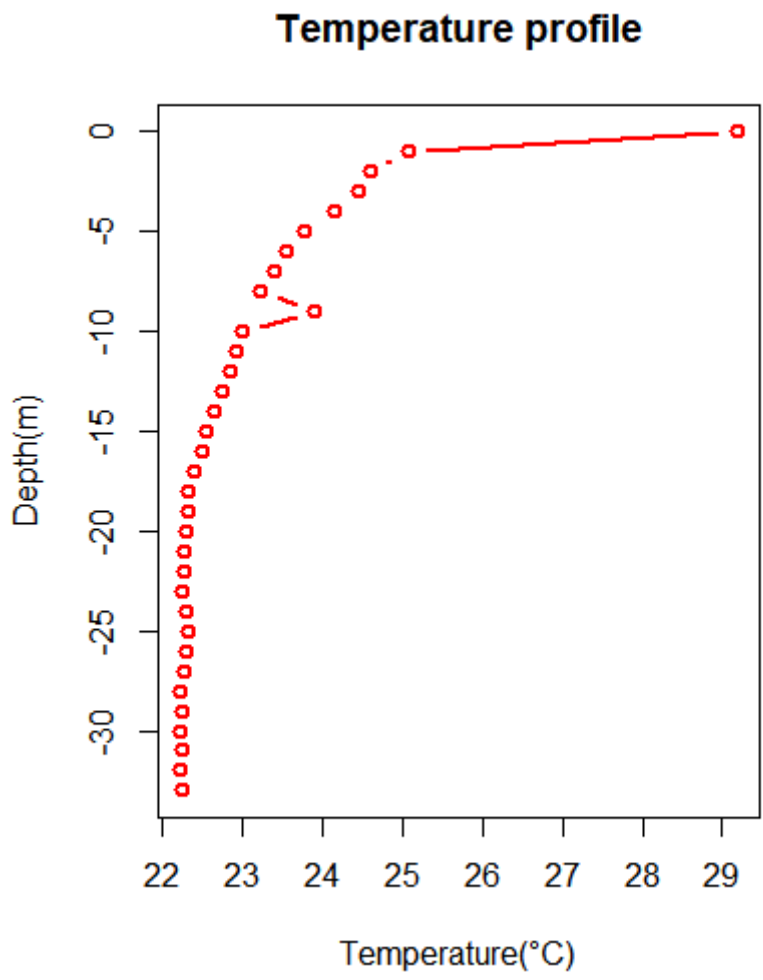


Figure 10. Temperature profile from 0-33 meter in the CDU reservoir.

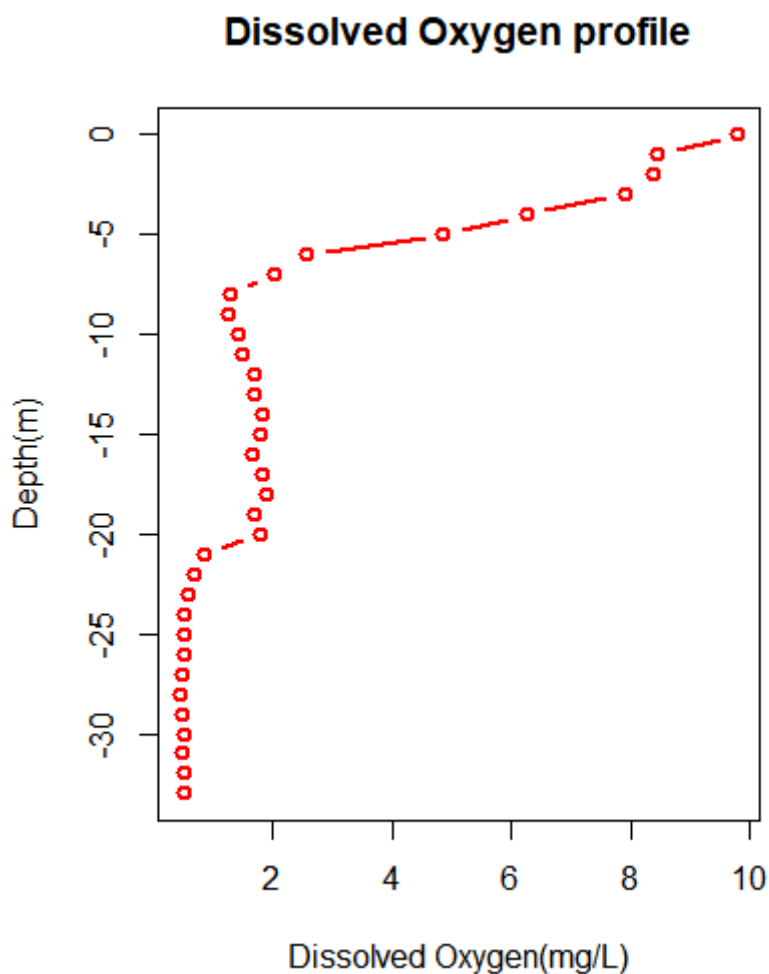


Figure 11. Dissolved oxygen (mg l^{-1}) concentration profile in the CDU reservoir.

4.2 VERTICAL DISTRIBUTION OF CH_4 CONCENTRATIONS IN THE WATER PROFILE

The concentration was increasing with depth and the highest concentration was located around 25 meters depth. The CH_4 concentrations ranged between 0.77 mg m^{-3} to 140 mg m^{-3} . The concentrations did not differ much in the upper layers down to 25 m where a peak in the concentration occurred. The table 5 shows the mean CH_4 concentration for each sampled depth. All samples can be found in the appendix in table 1. Each depth was sampled four times to ensure that the samples are not compromised by being exposed to air. No outliers were detected when analyzing the samples. The mean CH_4 concentration with standard deviation is plotted against depth.

Table 5. Mean concentration of CH₄ (mg m⁻³) for the water profile in front of intake for CDU with standard deviation.

Depth(m)	Mean CH ₄ (mg m ⁻³)	Std CH ₄ (mg m ⁻³)
0	5.9	0.76
5	0.77	0.22
10	0.48	0.069
15	0.38	0.053
20	2.2	0.053
25	137	21
30	4.6	2.7
35	10	2.8

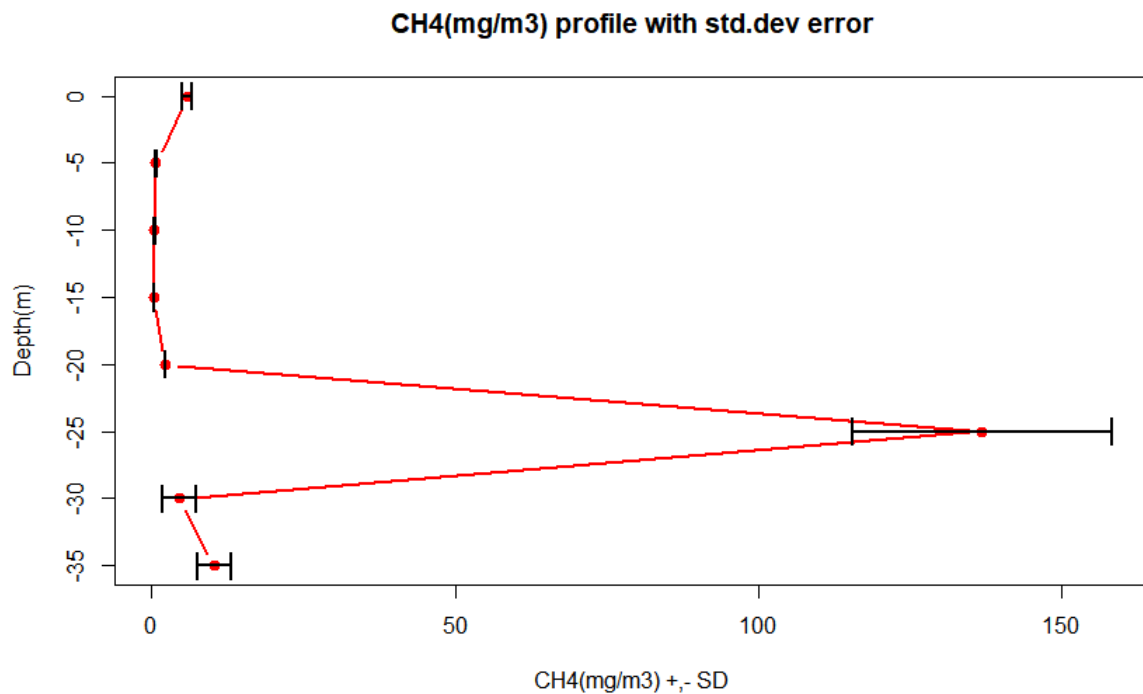


Figure 12. The mean methane concentration at CDU with standard deviation is plotted against depth

4.3 CH₄ CONCENTRATION AFTER THE DAM

The results show that there is a similar concentration of CH₄ in the water at 25 m depth and in the water that is discharged after the dam. The concentration of CH₄ in the air after the dam was 5.5 ppm compared to the ambient air concentration of 1.8 ppm that was found in front of the dam. The air concentration of CH₄ is only an indication of high concentrations in the out flowing water. The result from the water concentrations is calculated as a mean of the four samples taken at the exact same depth using the deep-water sampler.

Table 6. Mean concentration of CH_4 ($mg\ m^{-3}$) after the outlet for CDU 1 meter below the water surface with standard deviation.

Sampling height (m)	Mean CH_4 ($mg\ m^{-3}$)	Std CH_4 ($mg\ m^{-3}$)
1 (air)	3.32	0.0103
-1(water)	118	13

The depth of the intake water was unknown but was estimated to be around 25 meters. The difference of the CH_4 concentration at 25 meters depth before the dam and the CH_4 concentration after the dam was

$$C_{deg} = (137 - 118)(mg\ m^{-3}) = 19(mg\ m^{-3}) \quad (8)$$

The discharge from CDU varies from $2\ m^3/s$ to $7\ m^3/s$ during wetter periods with an average value of $5.5\ m^3/s$. At the day of the sampling the reservoir were at maximum capacity so by using the discharge with the release of $7\ m^3/s$ the daily release of CH_4 from the degassing process was $11.49\ kg_{CH_4}\ day^{-1}$ which corresponds to $390\ kg_{CO_2e}\ day^{-1}$.

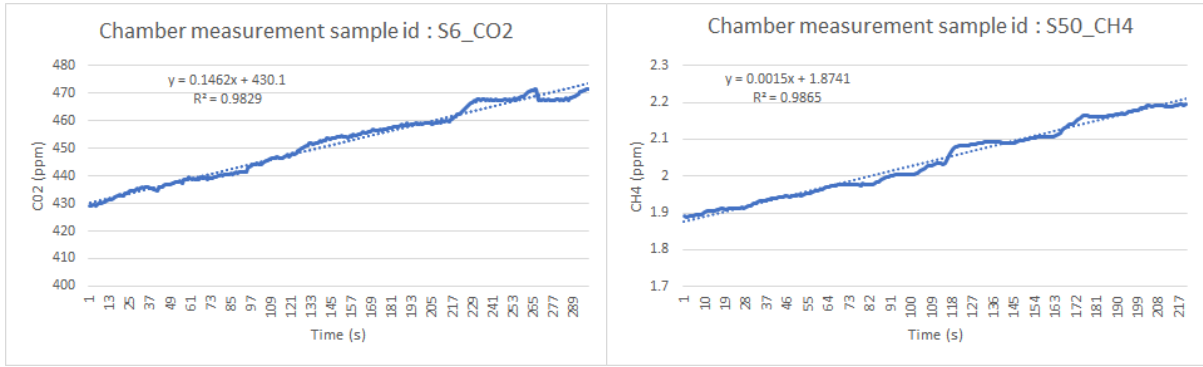
4.3.1 Gas-Exchange Coefficient

For the calculation of the K-value for CH_4 three replicas of chamber measurements and three replicas of surface CH_4 concentration was calculated to then use the mean value for the three measurements. The slopes of the regressions of pCO_2 against time were (0.15, 0.21, 0.06) [$pCO_2 * s^{-1}$] with corresponding R^2 -values of (0.98, 0.98, 0.91). For the measurements of CH_4 flux, the slope values were (0.0014, 0.0015, 0.0005) [$pCH_4 * s^{-1}$] and the corresponding R^2 -values were (0.99, 0.99, 0.97). All the R^2 -values were above 0.9, indicating that diffusive flux was measured. The measurements are shown in figures 13a-15b.

For the discrete measurements of the surface concentration of CH_4 and CO_2 three samples were taken at the same time as the chambers were deployed. For the calculations of the surface concentration the calibration curves for the $CO_2\ dry$ measurements were not able to be produced therefore only $CH_4\ dry$ concentrations could be calculated. For sample S6, S50 and S83 the results were, (213, 182, 157) [$CH_4\ dry$ (ppm)] and (7.9, 6.8, 5.9) [$CH_4\ dry$ mol(R)]. The temperature and the pressure from the time of each measurement were gathered from INMET's nearest meteorology station to Chapeu D'Uvas which was located in Juiz de Fora. The temperature was $25^\circ\ C$ and the atmospheric pressure was 911.7 (mbar). The Schmidt number which is used to normalize the K value was set for CH_4 to 560.17 (Jähne et al., 1987). From the water concentration, the k-value was calculated to (2.0, 2.6, 5.3)(CH_4) [$cm\ h^{-1}$] with a mean of 3.3 [$cm\ h^{-1}$]. The results are shown in table 7.

Table 7. CH_4 gas-exchange coefficient $kFCin$ (md^{-1} and ($cm\ h^{-1}$) for three replicas and the mean value of the samples, all samples are taken at the same location and the same time.

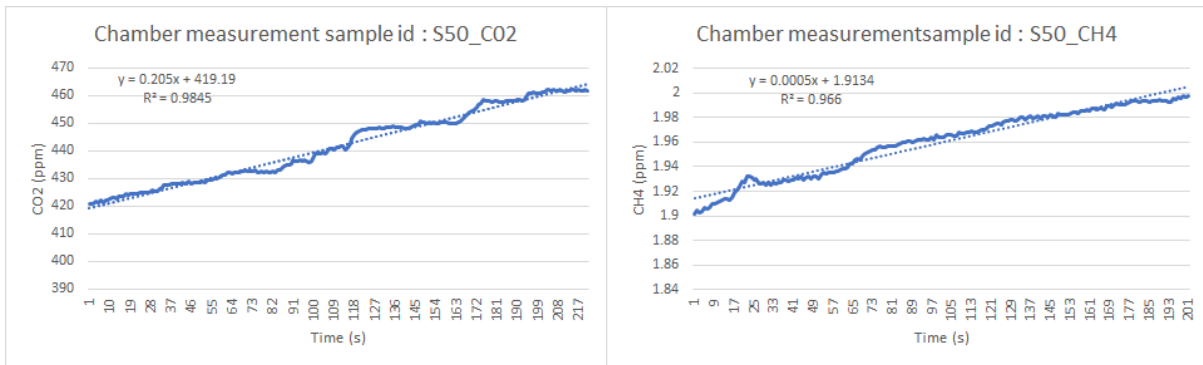
Sample	$kFCofCH_4$ ($m\ d^{-1}$)	$kFCofCH_4$ ($cm\ h^{-1}$)
S6	2.0	8.5
S50	2.6	10.9
S83	5.3	22.1
mean	3.3	13.8



(a) pCO_2

(b) pCH_4

Figure 13. Plots depicting chamber measurements of pCO_2 and pCH_4 plotted against seconds from sample S6 taken in front of the water inlet of Chapeu D'Uvas water reservoir. The slope line, corresponding slope value and R^2 -value is displayed in the graph.



(a) pCO_2

(b) pCH_4

Figure 14. Plots depicting chamber measurements of pCO_2 and pCH_4 plotted against time from sample S50 taken in front of the water inlet of Chapeu D'Uvas water reservoir. The slope line, corresponding slope value and R^2 -value is displayed in the graph.

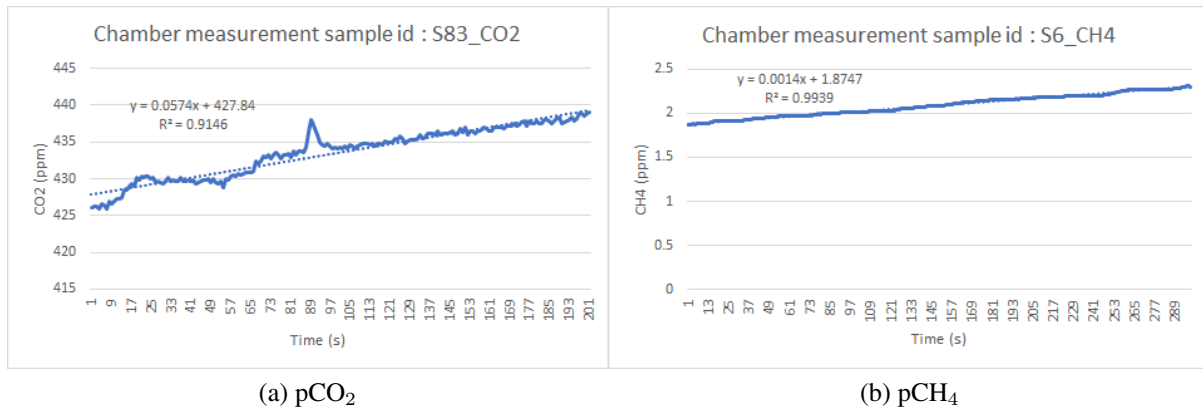


Figure 15. Plots depicting chamber measurements of $p\text{CO}_2$ and $p\text{CH}_4$ plotted against seconds from sample S83 taken in front of the water inlet of Chapeu D’Uvas water reservoir. The slope line, corresponding slope value and R^2 value is displayed in the graph.

4.4 MODELLED TEMPERATURE PROFILES

The results that will be presented here are the modeled temperature profiles for FUN using different calibrations. The measured temperature profiles that were used for training the model are displayed in figure 16 where the highest temperature is measured in red. The temperature profiles are measured at 5 different locations and from 15 separate months from 2017-2020. The figure shows the values being interpolated over the year. The highest temperatures were measured in December and the lowest temperatures in August. The water profiles were stratified during October to July and mixed during August and September. The temperature in the surface layers ranged from 21°C in August 2017 to 29°C in December 2018. The bottom temperature ranges from 20°C in February 2019 to 26.5°C in August 2019. The profiles from three different calibration ranges and setups will be presented in this section.

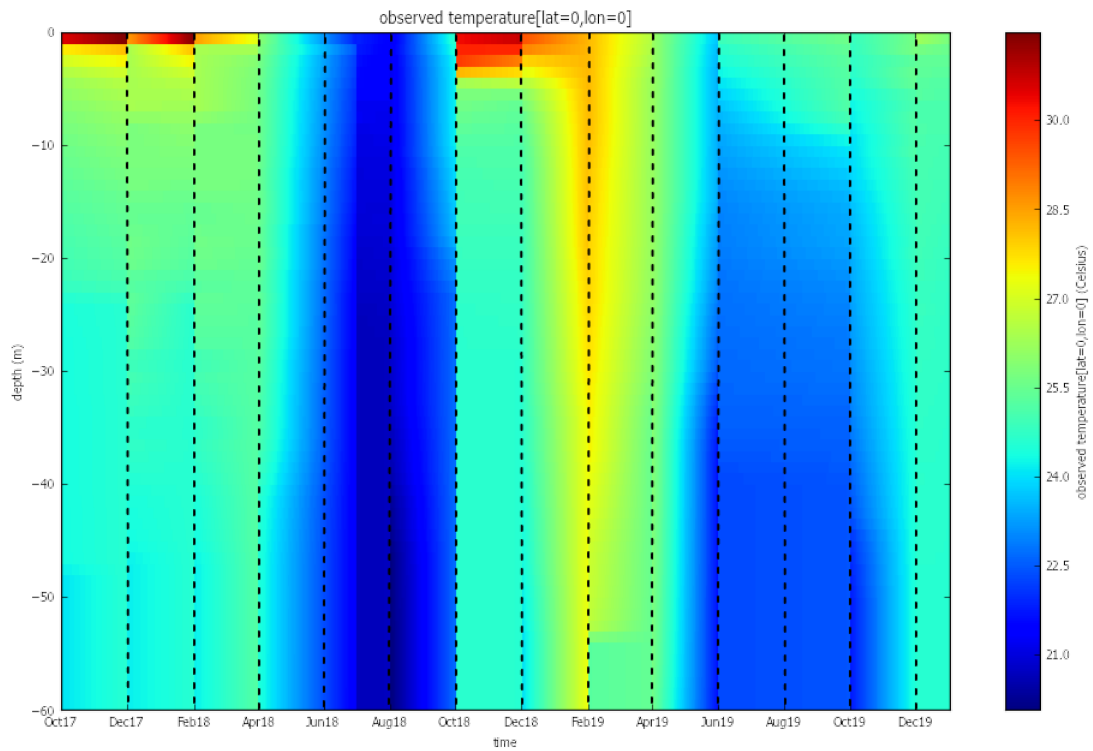


Figure 16. Measured water profiles from Funil is plotted against time. The water profiles consist of measurements from 2017-10-01 to 2020-01-01. The date of the discrete measurements is marked with a black dotted line. The values in between are interpolated.

In figure 17 the modeled temperature profiles are from the manually calibrated model with the scaling factors ($sf_{parameter}$) calibrated to $s_{heatflux} = 0.769$, $s_{SWR} = 0.962$, $s_{wind} = 1.424$, $s_{minkineticenergy} = 8.417 \times 10^{-1}$, $s_{e-folding} = 1.9$. The model shows periods of stratification and complete mixing. The range for the surface temperature is higher than the measured profiles were the highest temperature is 32 °C and the lowest 23.9 °C. For the bottom temperature the range is small (23.9 - 24.5 °C). The model accurately shows the seasonal variation of stratification and complete mixing. The model however overestimates the surface temperature and the temperatures for the depth down to 20 m for most profiles.

During manual calibration, the goal was to get the best possible model fit to the bottom water temperatures, because that is most relevant to O₂ consumption and CH₄ production in the sediments. The model fit was evaluated by looking at bias, RMSE and MAE. The model fit for the section 20-60 meter water depth with manual calibration was (RMSE=1.99 °C, MAE=2.52 °C, bias=-0.58 °C).

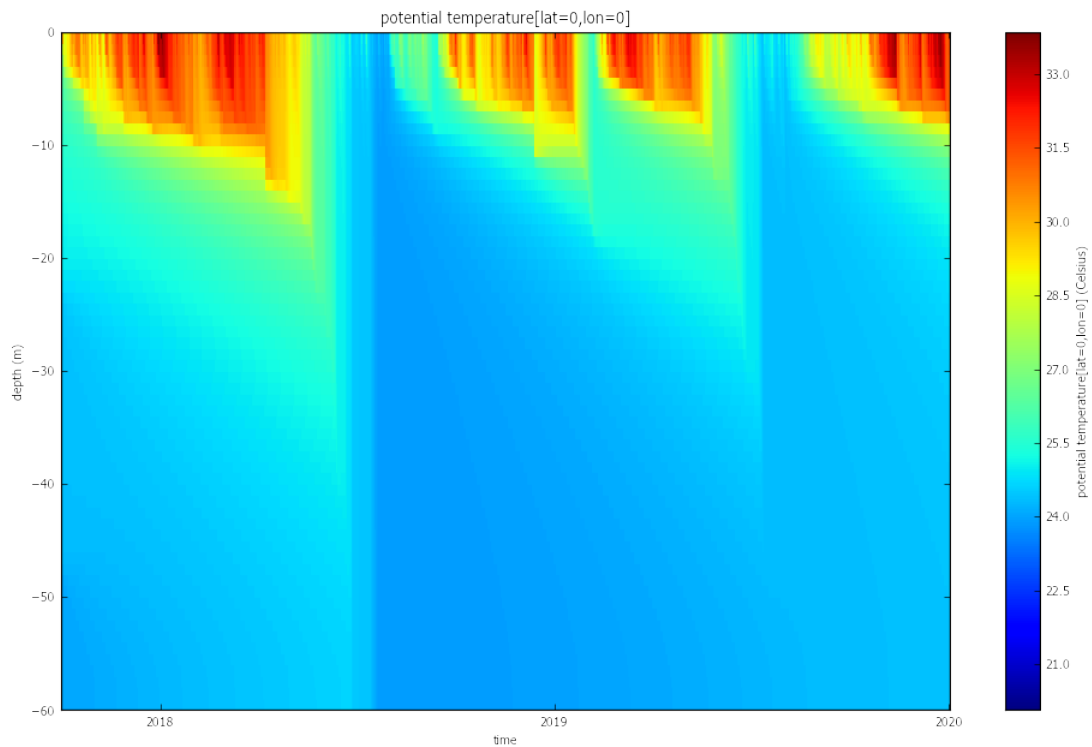


Figure 17. Modeled temperature profiles with manually calibrated scalar factors for Funil were temperature is plotted against time. The graph depicts temperature profiles for each day for the period from 2017-10-01 to 2020-01-01

In figure 18 the profiles from the model using the ACPy calibration are shown with the scaling factors ($sf_{parameter}$) calibrated to $s_{heatflux} = 0.828$, $s_{SWR} = 0.500$, $s_{wind} = 1.499$, $s_{minkineticenergy} = 2.664 \times 10^{-6}$, $s_{e-folding} = 1.002$. The model fit returns a RMSE of 1.54 for the entire profile. For the section 20-60 m, model fit was RMSE=1.58, MAE = 1.49 and bias = -0.58. The stratification during the warmer months was predicted by the model but was not as strong as for the measured data or the manually calibrated model and the profiles were completely mixed for long parts of the year. The modelled surface temperature was close to the measured surface temperature. When looking at the model fit for the first 20 meter (RMSE=1.47, MAE=1.24, bias=0.047) compared to the manual calibration for the same depth (RMSE=2.95, MAE=2.36, bias=-2.08), it becomes evident that the automated calibration results in a better fit for the surface temperature. The parameters from the first run resulted in values that were against the parameters boundaries. A second attempt with broader boundaries gave the results that tended to the extremes. The model fit for the ACPy model and the manually calibrated model for the entire profile and for the section 20-60 m can be shown in table 8.

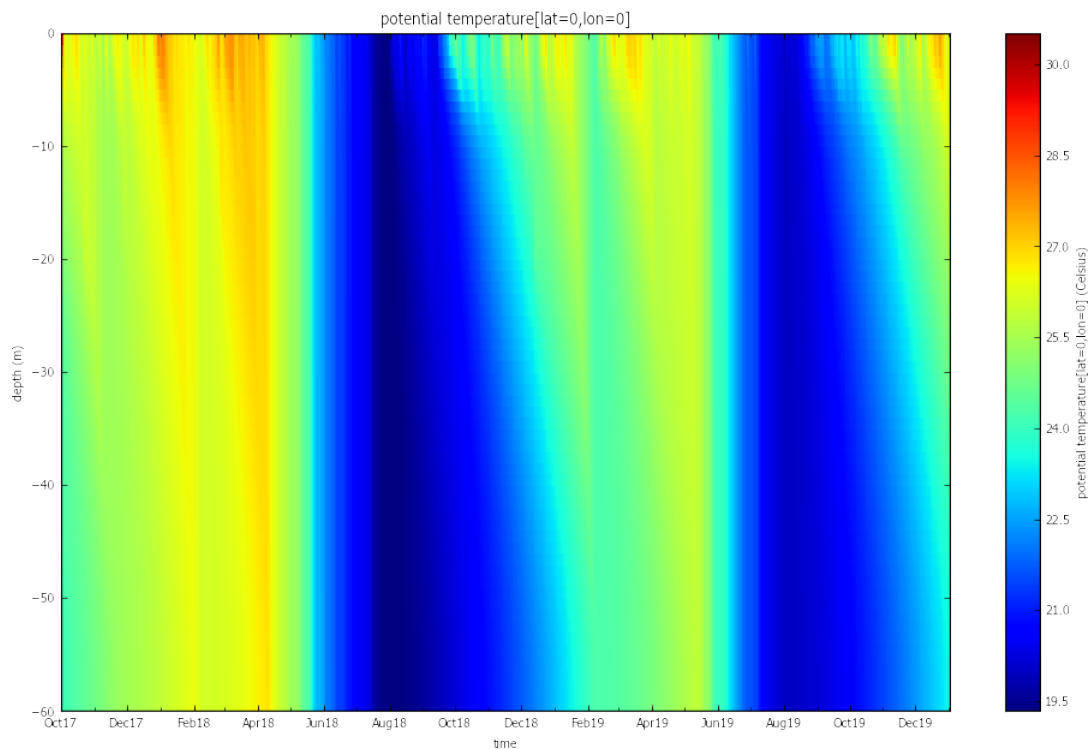


Figure 18. Modeled temperature profiles for Funil, with temperature profiles for each day during period 2017-10-01 to 2020-01-01 with ACPy calibration.

In figure 18 the profiles from the model using the ACPy calibration with the added air temperature scalar factor added are shown. The scaling factors were ($sf_{parameter}$) calibrated to $s_{heatflux} = 0.938$, $s_{SWR} = 0.802$, $s_{wind} = 1.499$, $s_{minkineticenergy} = 9.160 \times 10^{-6}$, $s_{e-folding} = 9.999$, $s_{airt} = 0.940$. The model fit gives a RMSE of 1.517 for the entire profile. For the section 20-60 m, model fit was (RMSE=1.459, MAE = 1.199, bias = -0.309). The modelled stratification and the mixing was similar to the ACPy run without the air temperature scalar. The surface temperature was close to the measured surface temperature. When looking at the model fit for the entire profile and the section 20-60 m, the ACPy model with air temperature scalar had the best fit out of all the models. The model fit can be found in table 8.

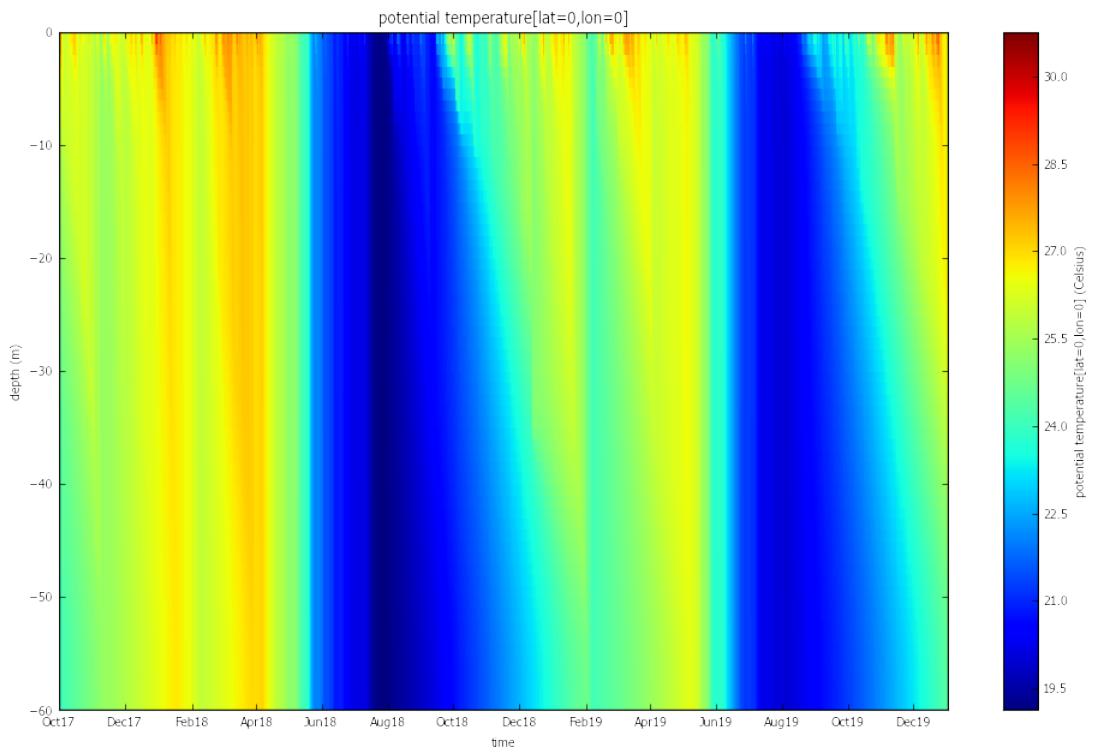


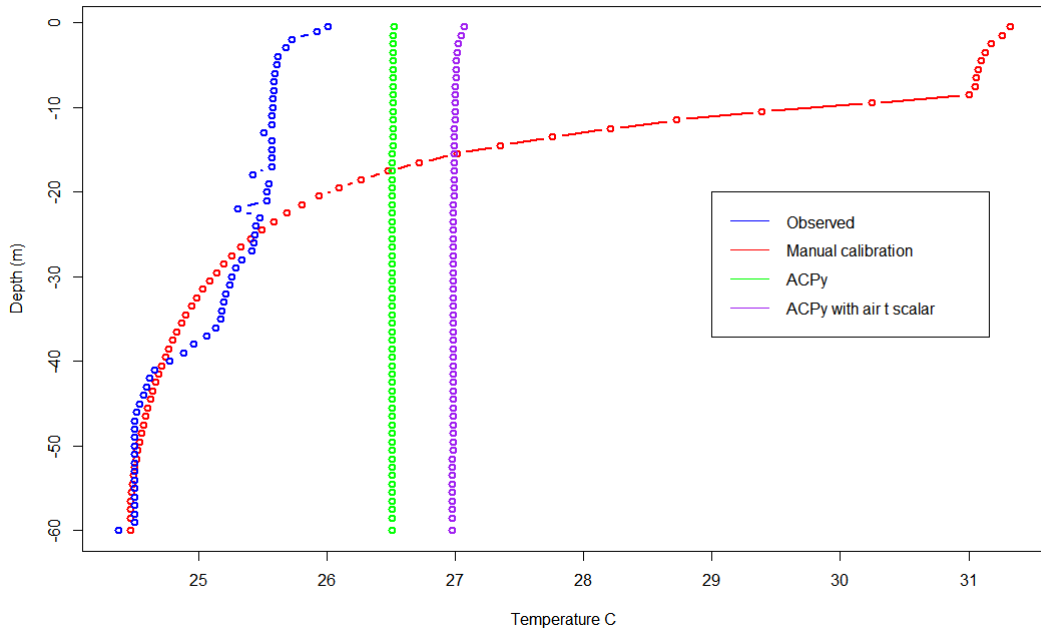
Figure 19. Modeled temperature profiles for Funil, with temperature profiles for each day during period 2017-10-01 to 2020-01-01 with ACPy calibration and a added scaling factor for air temperature

Table 8. Model performance for the entire calibration period 2017-2020 for the ACPy with air t scaling factor, the ACPy calibration and the manual calibration

Calibration interval	Model statistic	Value ACPy airt	Value ACPy	Value Manual
0-60 (m)	Bias (°C)	-0.175	-0.413	-1.094
	MAE(°C)	1.234	2.376	5.652
	RMSE(°C)	1.517	1.541	2.377
20-60 (m)	Bias (°C)	-0.309	-0.590	-0.584
	MAE(°C)	1.199	2.526	1.402
	RMSE(°C)	1.459	1.589	1.995

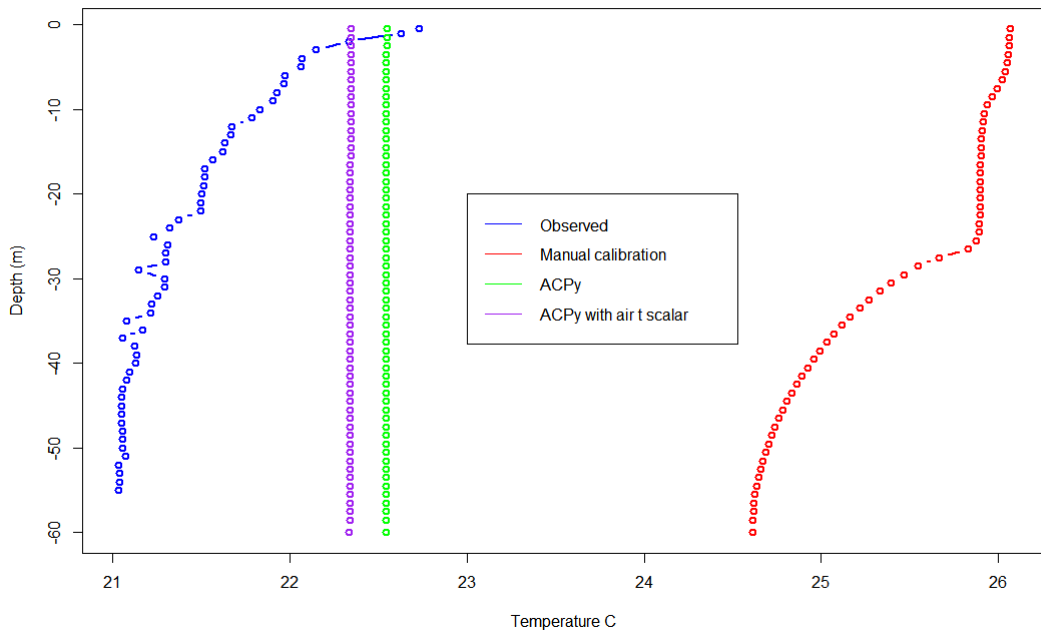
The figures in figure 21 shows the measured profiles from 2018. The figures in figure 23 shows the measured profiles from 2019 and they are plotted against the manually calibrated profiles, the ACPy profiles and the ACPy calibration with the added air temperature scalar. The measured profiles are from the month but from the gathered data the exact day is not specified. But the data from the model is taken from the first day of each respective month. The modelled profiles are from the sampling location PB80. The profiles were measured every two months and are compared with modeled profiles for the months February, April, June, October and December. The manual calibrated model in red predicts higher surface temperatures than the measured profiles and the ACPy calibrated models. For the depth below 20 m the manually calibrated model generally predicts temperatures close to the measured profile when the measured profiles show clear stratification.

Temperautre profile 2018-04-01 with measured,manual calibrated, ACPy, ACPy with air T scaling factor



(a) 2018-04-01

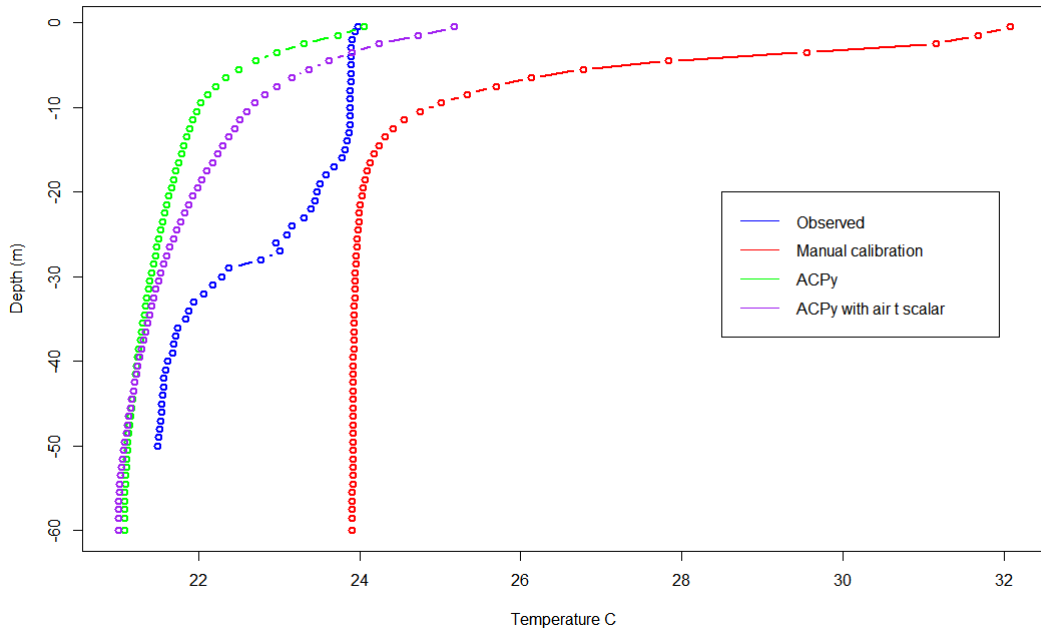
Temperautre profile 2018-06-01 with measured,manual calibrated, ACPy, ACPy with air T scaling factor



(b) 2018-06-01

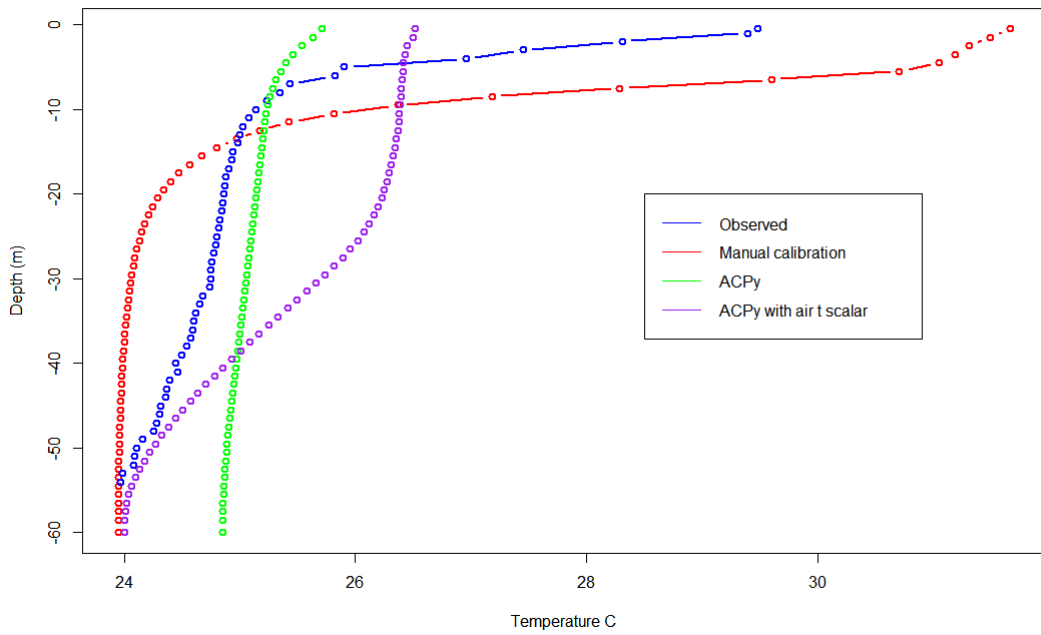
Figure 20. 2018 Measured Temperature profile (blue), modeled profile using the automated calibration (red) ACPy calibration (green) and ACPy calibration with air T scalar factor (purple).

Temperautre profile 2018-10-01 with measured,manual calibrated, ACPy, ACPy with air T scaling factor



(a) 2018-10-01

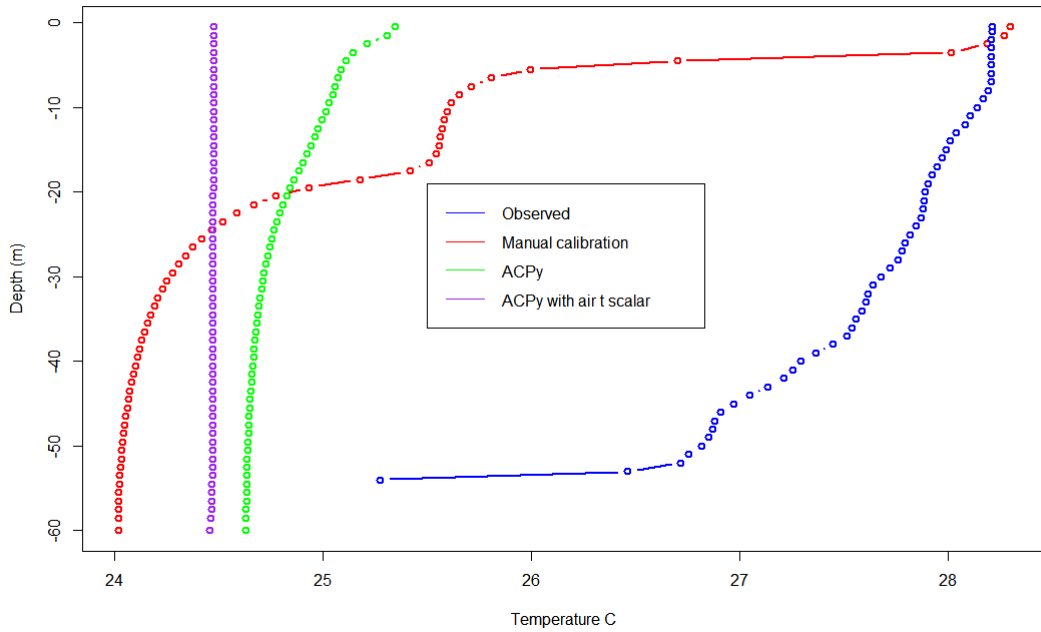
Temperautre profile 2018-12-01 with measured,manual calibrated, ACPy, ACPy with air T scaling factor



(b) 2018-12-01

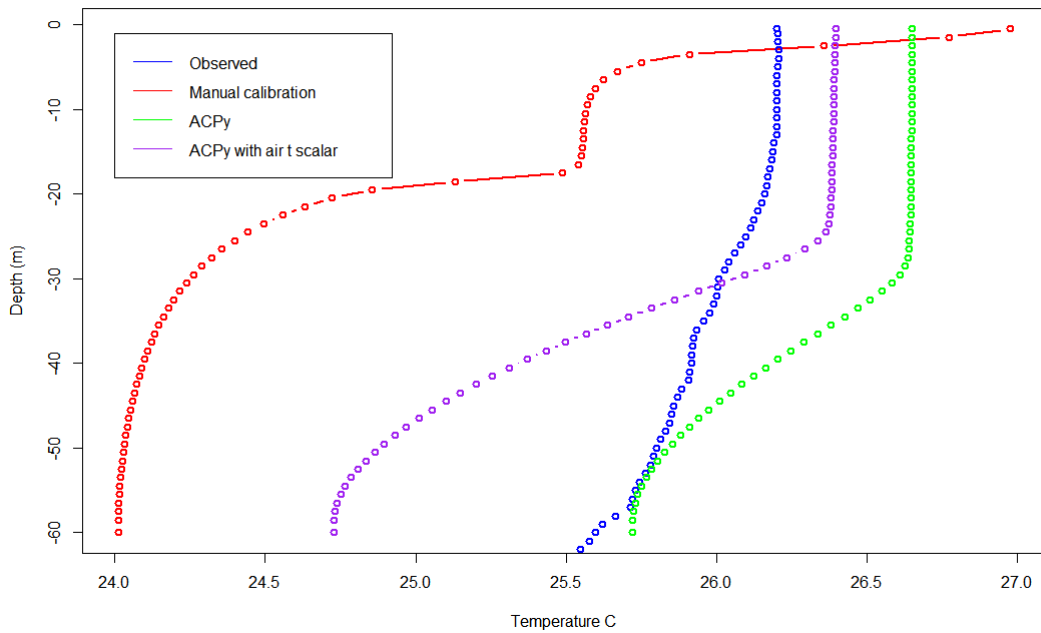
Figure 21. 2018 Measured Temperature profile (blue), modeled profile using the automated calibration (red) ACPy calibration (green) and ACPy calibration with air T scalar factor (purple).

Temperautre profile 2019-02-01 with measured,manual calibrated, ACPy, ACPy with air T scaling factor



(a) 2019-02-01

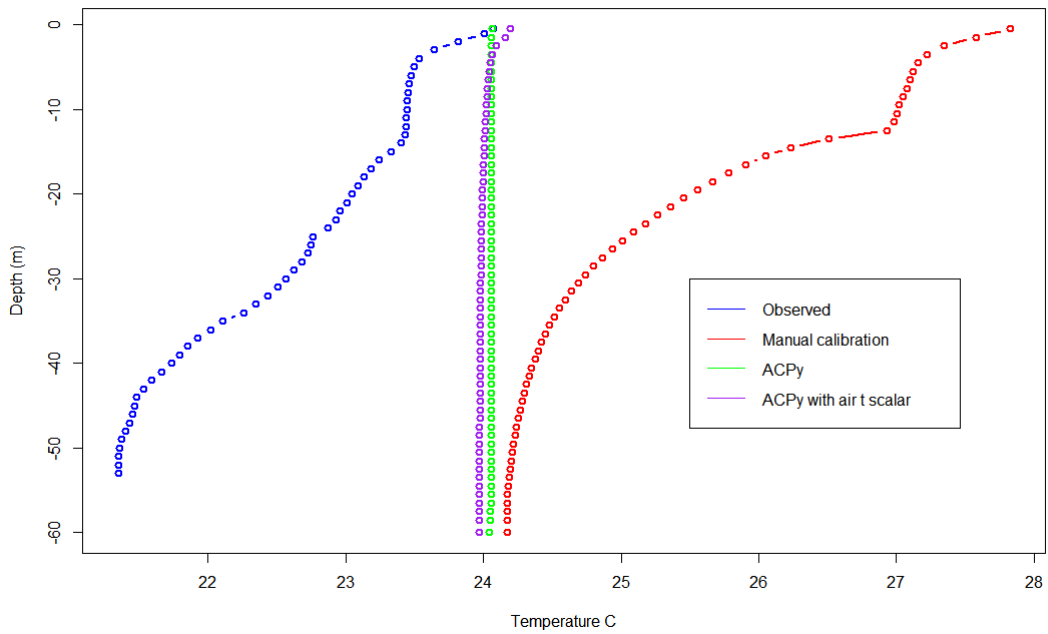
Temperautre profile 2019-04-01 with measured,manual calibrated, ACPy, ACPy with air T scaling factor



(b) 2019-04-01

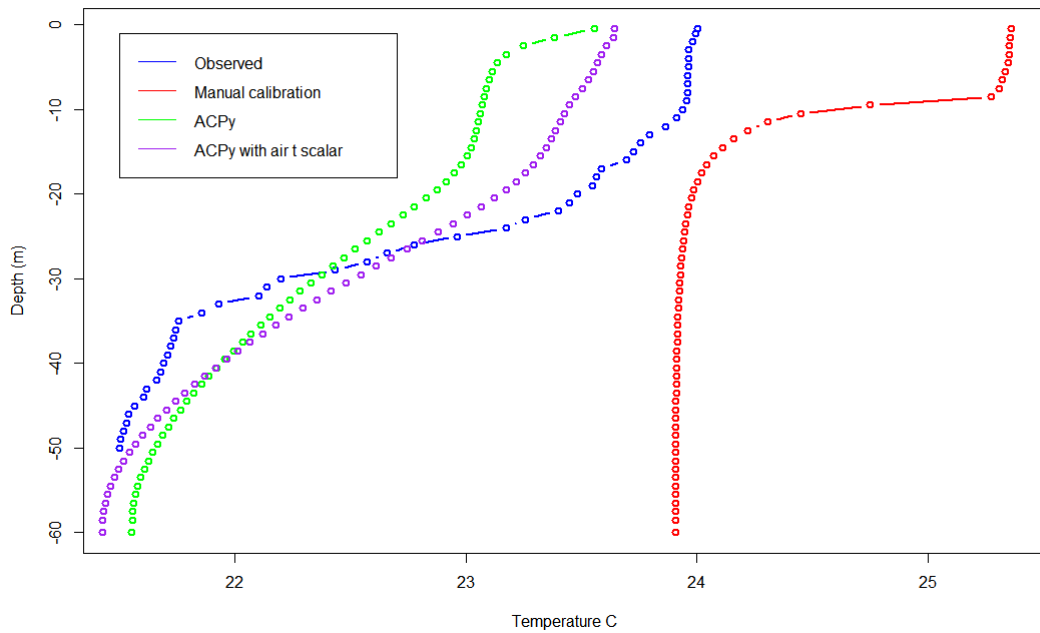
Figure 22. 2019 Measured Temperature profile (blue), modeled profile using the automated calibration (red) ACPy calibration (green) and ACPy calibration with air T scalar factor (purple).

Temperautre profile 2019-06-01 with measured,manual calibrated, ACPy, ACPy with air T scaling factor



(a) 2019-06-01

Temperautre profile 2019-10-01 with measured,manual calibrated, ACPy, ACPy with air T scaling factor



(b) 2019-10-01

Figure 23. 2019 Measured Temperature profile (blue), modeled profile using the automated calibration (red) ACPy calibration (green) and ACPy calibration with air T scalar factor (purple).

Figure 24 shows the profiles from 2019-12-01 in a upscaled figure, the profile are from the sampling location

PRB 80. These are the profiles that the manually calibrated model best predicts for the lower depths. The surface temperature for the observed profile in 2019 is 26.3 °C and the surface temperature for the manually calibrated modeled in 2019 is 31.9 °C. For the lower depths the measured and manually calibrated modeled for 2019 is 23.4 °C and 23.9 °C and for 2020 it is 24.4 °C and 24.0 °C. From 20 m depth the model predicts the temperature with mean error of 0.15 °C.

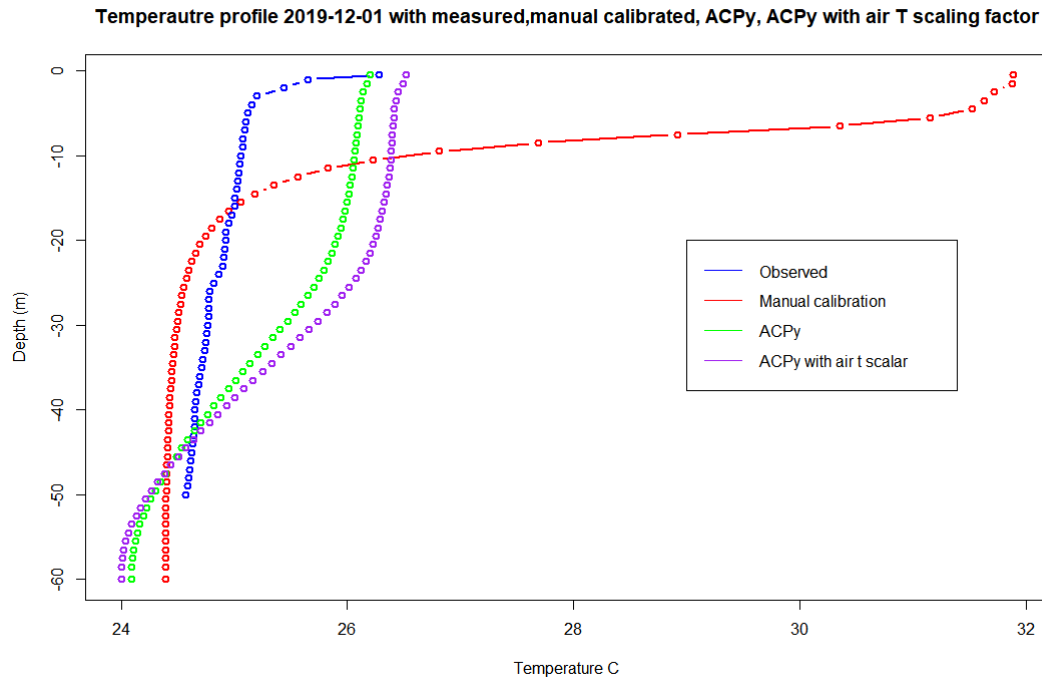


Figure 24. Measured Temperature profile (blue), modeled profile using the automated calibration (red) ACPy calibration (green) and ACPy calibration with air T scalar factor (purple) from Funil 2019-12-01

In figure 25, 26 and 27 all the profiles from the ACPy model with the air t scaling factor are compared with the observed temperatures for different depths with the RMSE. The RMSE ranges from 1.87 at 1 m to 1.3 at 20 m and the average for the RMSE is 1.5. From the figures the yearly variation in temperature can be seen with the lowest temperature in the June-August and the highest around December. The figures are created down to 50 m since there only 5 measured profiles that are deeper than 50 m.

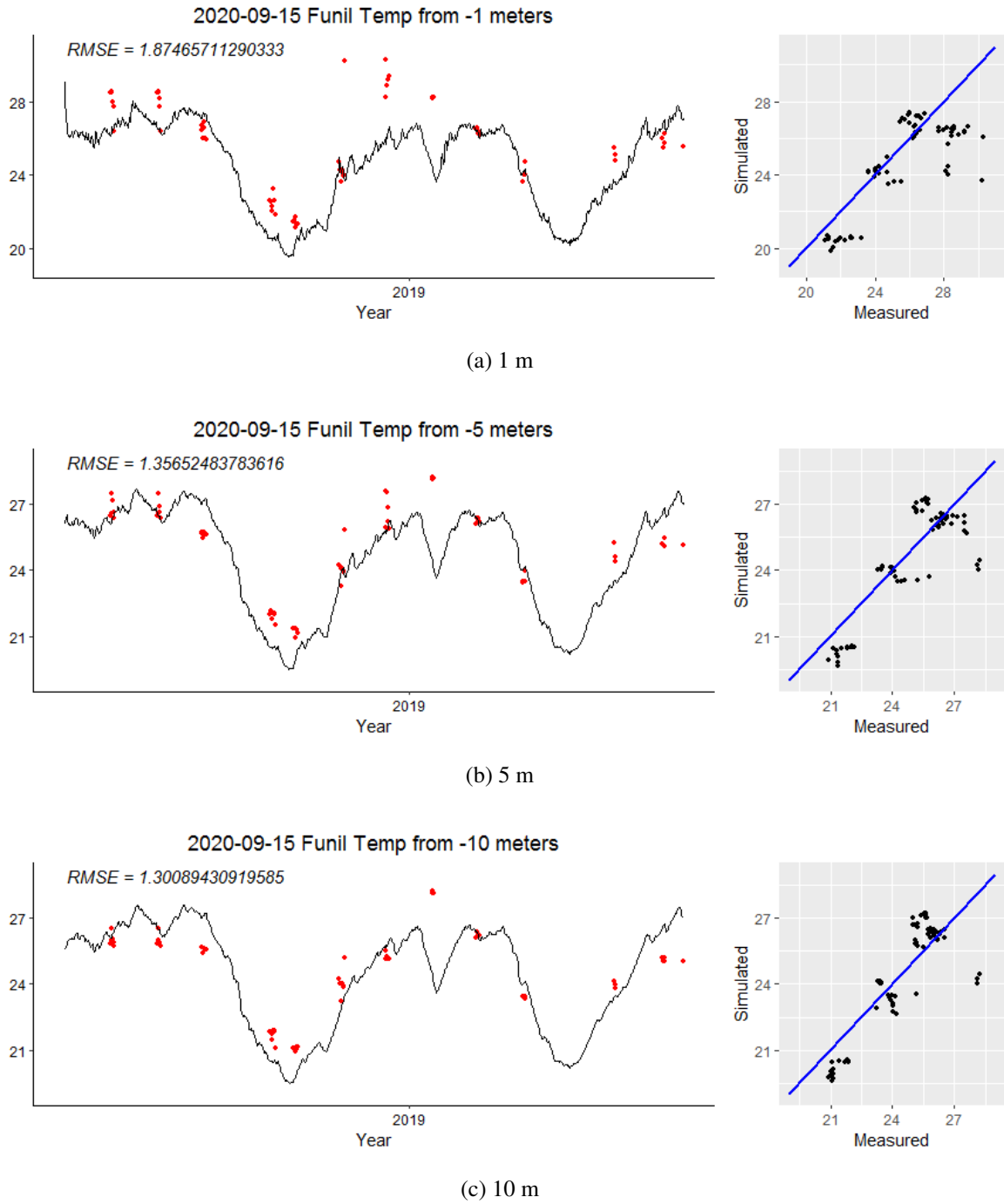
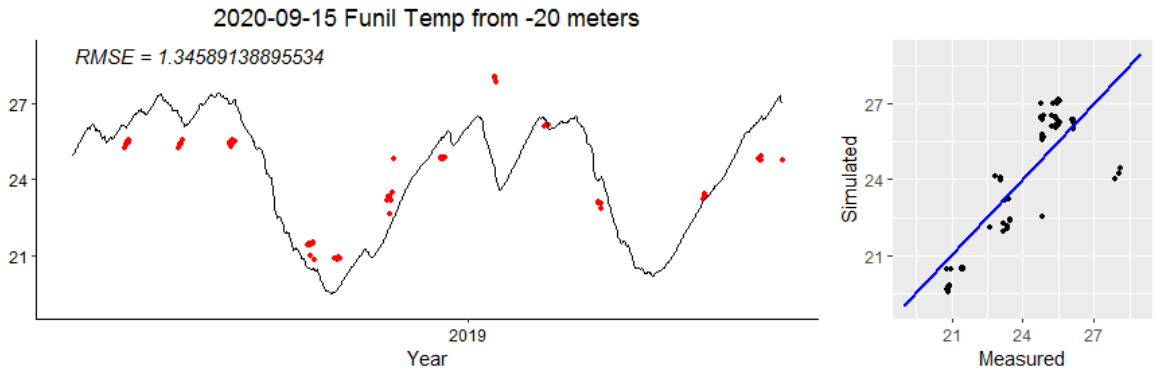
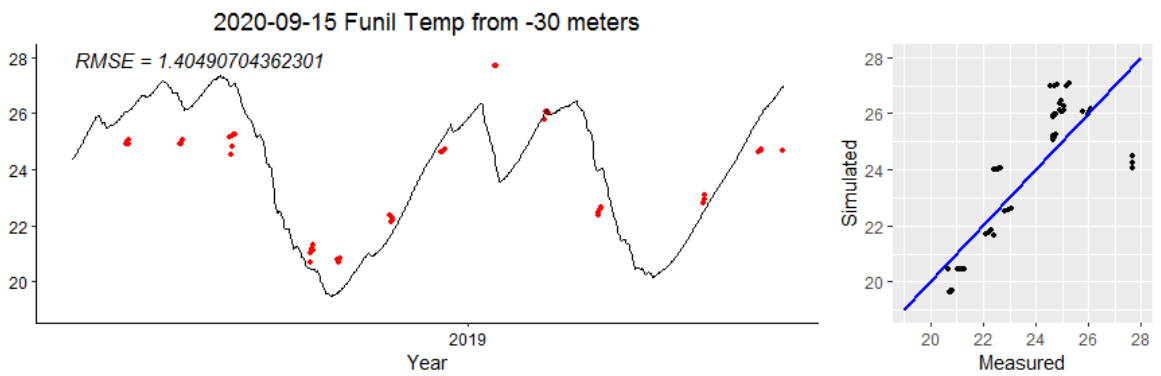


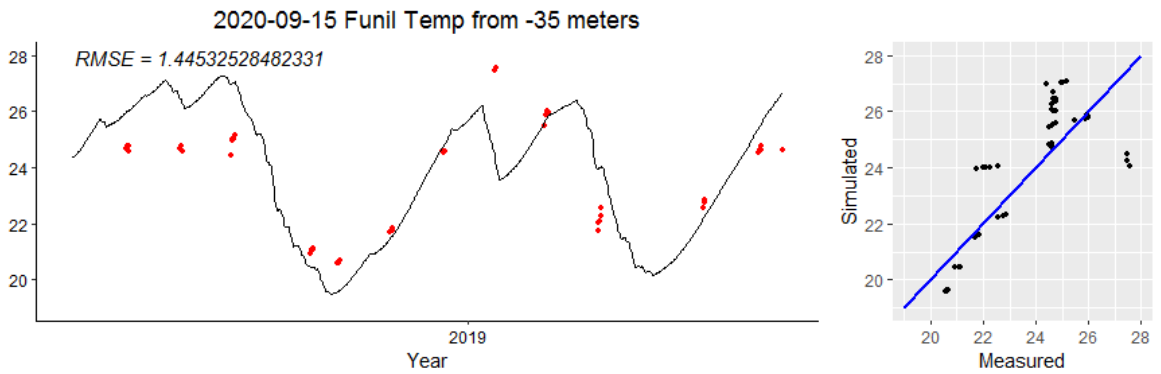
Figure 25. Modeled temperatures from ACPy calibration with air temperature scaling factor and measured temperatures for meters 1,5,10.



(a) 20 m

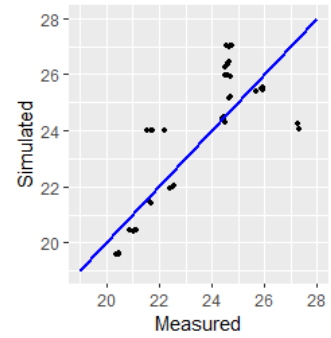
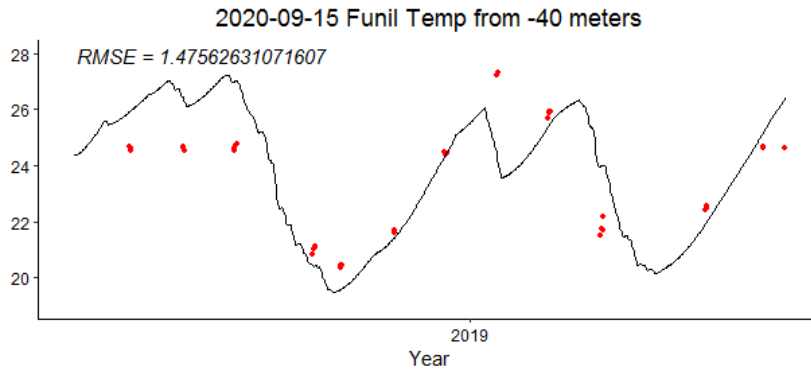


(b) 30 m

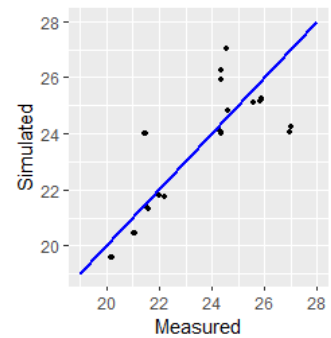
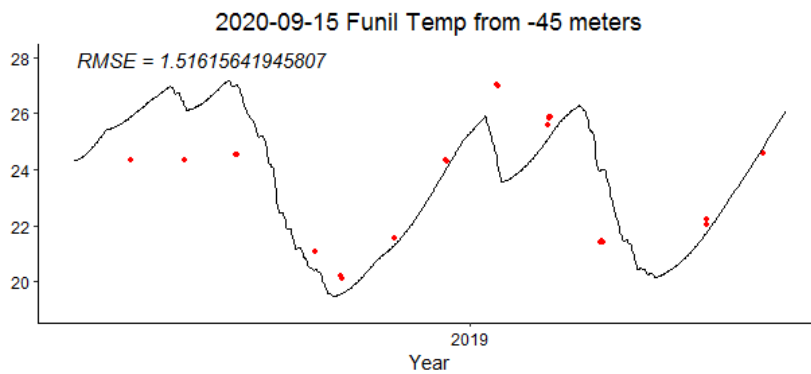


(c) 35 m

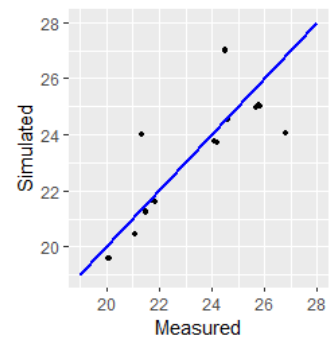
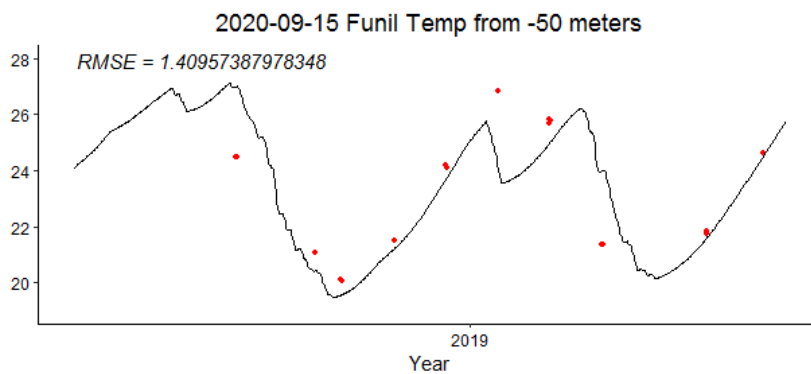
Figure 26. Modeled temperatures from ACPy calibration with air temperature scaling factor and measured temperatures for meters 20, 30, 35.



(a) 40 m



(b) 45 m



(c) 50 m

Figure 27. Modeled temperatures from ACPy calibration with air temperature scaling factor and measured temperatures for meters 40, 45, 50

5 DISCUSSION

5.1 MEASUREMENTS AT CHAPEU D'UVAS.

From the figure 12 the CH₄ concentration for the surface water was $5.9 \pm 0.76 \text{ mg m}^{-3}$, the highest concentration in the profile were at 25 m depth where the concentration where $140 \pm 21 \text{ mg m}^{-3}$, these values are in the range of what is found in the literature (Gu erin et al., 2006). The CH₄ concentration of the out flowing water was $120 \pm 13 \text{ mg m}^{-3}$. This CH₄ will be released into the atmosphere in the form of CH₄ through diffusion or as CO₂ after going through methanogenic oxidation until the water downstream has reached equilibrium with the atmosphere. To estimate the emissions from the discharge for this example the daily emission from CH₄ is 11.49 kg d^{-1} or $390 \text{ kg CO}_{2e} \text{ d}^{-1}$. The assumptions made for this example is that the outflow is estimated to $7 \text{ m}^3 \text{ s}^{-1}$ based on the conditions of the day when the samples were taken. An estimate of the level for the inlet is also made that the water inlet is taking in water with the concentrations found at 25 meters depth and all CH₄ is released into the atmosphere and not converted to CO₂. This estimate can be backed since the concentrations of the out flowing water ($120 \pm 13 \text{ mg m}^{-3}$) are similar to the concentrations measured at 25 m depth ($140 \pm 21 \text{ mg m}^{-3}$). From measurements done by previous studies in Chapeu D'Uvas $390 \text{ kg CO}_{2e} \text{ d}^{-1}$ is a relative high value when compared to the mean diffusive CH₄ emissions in Chapeu D'Uvas (Linkhorst, 2019), of $80 \text{ mg C m}^{-2} \text{ d}^{-1}$ or $760 \text{ kg CO}_{2e} \text{ d}^{-1}$ for the whole reservoir. With these estimations the degassing that degassing corresponds to 34% of diffusive CH₄ emission. When comparing the calculated k-values 3.3 m d^{-1} (table 7) with the k values from another sampling camping of 4 m d^{-1} (Parana ba et al., 2018) the values were similar. Since the calibration for the CO₂ was not done before the field campaigns had to be aborted, the contribution of CO₂ to degassing emissions cannot be calculated from the collected samples and therefore the estimate represents an underestimate.

By using estimations from two other studies, one where the estimate of the CO₂ emissions from the turbine degassing process is 100% of the downstream concentration (Li et al., 2015), and one of the downstream concentrations in turn are estimated to 15% of the diffusive surface fluxes, (Kemenes et al., 2011). Using the CO₂ diffusive surface flux of $392\text{--}1000 \text{ kg d}^{-1}$ in CDU from (Linkhorst, 2019). With these estimations the degassing of CO₂ could range between $59\text{--}150 \text{ kg CO}_2$ adding these values to the measured CH₄ emissions the total degassing emission is $490 \text{ kg CO}_{2e} \text{ d}^{-1}$, with the estimated total C emission of $35 \pm 0.3 \text{ t CO}_{2e} \text{ d}^{-1} \pm \text{SEM}$ (standard error of the mean) for CDU made in the study for April–May 2016. The degassing process would stand for only 1.4 % of the total emission not counting the downstream emissions. This estimate is very hypothetical and many assumptions are made. Another approach is looking at the literature to find studies that have measured the relation between CO₂ and CH₄ degassing for tropical reservoirs, I were not able to find any studies as this. The closest one I found was a study by that had measured CO₂ degassing from the turbine of $930 \pm 1053 \text{ g m}^{-3} \text{ s}^{-1}$ and the degassing of CH₄ to $-9.8 \pm 1.2 \text{ g m}^{-3} \text{ s}^{-1}$ (Rodriguez and Casper, 2018). These values are not enough to make a estimate. For the calculation of the daily emission of CH₄ from the outflow of water there are a lot of uncertainties to take into account when estimating the emissions released the atmosphere the biggest one is the assumption of the CO₂ emissions from degassing. So, by only including the estimated CH₄ emissions the underestimated contribution of the degassing process from CDU is 1.1% of the total GHG emissions from the drinking water reservoir CDU. When comparing CDU with other reservoirs a study report emissions from the degassing process ranging in magnitude from $2.7 \text{ t CO}_{2e} \text{ d}^{-1}$ to $1378 \text{ t CO}_{2e} \text{ d}^{-1}$ for two Brazilian hydropower reservoirs (dos Santos et al., 2017). The CH₄ emission from the degassing process of CDU shows low values in comparison with these reservoirs.

A important characteristics of CDU that impact the quantity of CH₄ is that CDU is a drinking water reservoir and the discharge of the water is less turbulent since most of the water leaves the reservoir to the supply system and not through any turbines. With the low discharge of $7 \text{ m}^3 \text{ s}^{-1}$ to the downstream river it would probably be little degassing emissions at CDU even if the CH₄ concentrations were higher. With less turbulent discharge less of the CH₄ is exposed to the air and diffuses. The concentration of CH₄ might also be lower since the water is oligotrophic with less organic matter and less productivity in the water compared to a reservoir that is eutrophic.

The water profile showed stratification of the water in the top layer of the water column (10). The oxygen levels were shown to decrease to anaerobic levels for the deeper parts of the water column. From the literature this would imply that there would be higher CH₄ levels in the lower parts of the water column. After analyzing the CH₄ concentrations from the water samples this could be shown for the water sample taken at 25 m depth but for the sample taken at 35 m a lower concentration was found. From the measurements at 26 m a drop in conductivity from 31 S cm^{-1} to 24 S cm^{-1} was recorded and a peak in turbidity from 16 FNU to 44 FNU, indicating that there is a different water mass compared to the water at deeper depths. The lower concentrations of methane at the bottom can also be due to contamination of the samples, since the transfer from the DWS to the syringes is very

delicate and there is the possibility that the sample is exposed to the air which quickly lowers the concentration in the sample. However, the replicate samples from the same depth showed similar values that indicates that the sampling worked well and can be reproducible. Another thing to take into account is the accuracy of the concentration of CH₄ since the DWS only was tested that it did not take in water from other depth than the sampled. The DWS is built to not leak gas, all the valves and syringes have been tested for gas leakage and been shown to be airtight for at least 24 hours. This is the reason why the normal Ruttner samplers that also were available not were viable to use for the deep-water sampling of CH₄. For the measurements after the outlet, there were still a high amount of CH₄ in the water. One thing to note is that there is a possibility that the surface water coming from the spillway (seen in figure 7) is mixing with the outlet of the water with the higher concentration of CH₄, this would then lower the CH₄ concentration of the water found after the outflow and the measured CH₄ concentration could then be lower as a result of this instead of the CH₄ begin released to the atmosphere.

The sampling campaign for Chapeu D'Uvas was successful in collecting CH₄ deep-water samples and the method can be replicated to analyze the CH₄ concentrations for other reservoirs. The result of the CH₄ concentration are in the range of other CH₄ concentrations measured during other periods in CDU. The degassing process was estimated to correspond to only for 1.4 % of the total emission from CDU (CO_{2e} d⁻¹) when comparing with the total daily emissions (Linkhorst, 2019).

5.2 MODELLED TEMPERATURE PROFILES

The best-fitted calibrated model produced a consistent data set of daily profiles from 2017-2020 with a RMSE of 1.517 °C (Table 8). The model with best model fit was calibrated with the ACPy calibration with a added scaling factor to the air temperature. When using the scalar factors from the ACPy, was possible to predict the seasonal changes in temperature for the entire profile (Figure 25-27). The first ACPy calibration without air temp scalar probably did not generate good model fit because of the low number of measured profiles from the reservoir and the fact that the meteorological data used in the model, including air temperature, were measured around 20 km from the reservoir. For the first ACPy calibration a scalar factor for the short-wave radiation of 0.5 was derived. The ACPy calibration pushed to lower the surface temperatures which the manual calibrated model was predicting higher than the measured (Figure 24). This could be the result of the exact date of the measured temperature profiles are not known. From the data file they are stated to have been measured the first of every month but if the measurement is off by one day it can affect the model. If a measured profile is measured one day when it was cloudy but in the model is paired with a day when there were no clouds and high SWR the model will predict wrong temperatures. Since the most important temperatures for the further purpose of predicting bottom water oxygen and methane are the ones in the deeper water layers the scalar factors were then calibrated manually to get a better model fit for section 20-60 m. The manual calibration generated the profiles in figure 24 and in the figures 21 and 23 (red line), and the model fit for the manual calibration were not as good as the ACPy calibration for the entire profile but slightly better for the section 20-60 m (Table 8). The ACPy calibrated model was able to produce water columns with temperatures profiles that were in the range of the measured water columns and were able to capture the seasonal changes when comparing the output of the model with the measured profiles in figure 21 and 23. The model fit varied from the different months, the reason for this can probably again be attributed to the low number of measured temperature profiles and that they were measured only every other month, paired with the distance to the meteorology station. The main differences of the measured water columns and the modeled were that the model predicted higher values for the surface temperature and down to 10-20 meter. The main problem with the manually calibrated model was that it predicted too high surface temperature values. To try to correct for the high surface temperatures an assumption was made that the model predicted too high air temperatures as a result of the SWR data not being completely representative due to the distance from the meteorology station to the reservoir. Instead of letting the ACPy affect the SWR data to much a scalar factor for the air temperature where instead applied and calibrated between 0.8-1.2 resulting in more realistic values for the SWR scaling factor. The new ACPy calibrated model gave the best model fit for the whole profile (Bias=-0.175 °C, MAE=1.234 °C, RMSE=1.459 °C) and where able to predict the seasonal changes in stratification and mixing of the profile (Figure 21,23).

The temperatures for the lower depths were able to be predicted with a mean RMSE of 1.5 °C (Figure 25-27). For the purpose of using these data sets for modelling CH₄ production it is most important to have accurate temperatures in the lower depths since its their anaerobic conditions is first formed. It is also important that the model

is able to predict the seasonal changes in temperature, mixing and stratification which the model seems to be able to do when looking at the heat map in figure 19. The stratification is an important characteristic of the water profile since it gives information about stratified layers that can contain the higher CH₄ concentrations.

One part of the explanation that the model does not predict the stratification with more accuracy is likely because of the difference in the input data that was used. In the original model for Erken the water profiles were from one point in the lake and the data had longer time periods. The temperature profiles that were available for Funil were sampled at different locations in the reservoir which had different depth and temperature. This made the model calibrate from water profiles that were of different depth and characteristics. Another potential error is that in the measured profiles the date for the sampling is always the first of the month. If this is not the correct date for the measurements but they are sampled another day in the month this will affect the model output since it assumes it is the correct meteorology data for that day and adjust the rest of the model using those values. This is especially important when there is a limited amount of measured profiles throughout the year. Considering these potential sources of error, the model does manage to predict the temperature profile rather well. The model could potentially be used for other reservoirs in Brazil. How well the model would predict the temperature profile comes down to how big the data set of historical profiles are and how close the input data from meteorological station is to the measured profiles. The more data and the closer the meteorological data increases the potential of the ACPy to generate good scalar factors. The calibration could be helped by performing sight depth measurements at the reservoir to provide an estimate of the e-folding depth. Another way to try to improve the ACPy is to only calibrate the profile from 10-60 meter by removing the surface temperature down to 10 m for the profiles used for the calibration. This could remove the problem that occurs when the ACPy is trying to minimize the error of the high temperatures given in the surface layers.

Some temperature profiles give good predictions for the lower depths and can be used to estimate and model the oxygen consumption and the CH₄ production. The results generated from the model with the current calibration could be used to proceed with the next two steps of the model approach since there is a consistent data set of daily temperature data that captures seasonal stratification and mixing. Including the empirical model of oxygen demand and the CH₄ formation as a function of temperature and with a hourly time step could give an indication of the CH₄ formation. To get more accurate results the model could be calibrated further by removing the top 10 meters of the profiles as a way to try to improve the predictions in the bottom layers. Another improvement could be to include more measured profiles than the ones that were able to be gathered needs to be used as input data for the model. The calibration should focus on trying to get a better model fit for the lower depths but there is also a need to get good temperatures in the surface, since there can be sediments in shallow regions as well. In studies of CH₄ ebullition it has been shown that the shallow areas contribute a significant and in many times dominant share of the total CH₄ ebullition (Linkhorst, 2019).

5.3 POTENTIAL MITIGATION

To ensure that the gas emission from the degassing process is as low as possible the gas concentrations from the intake levels should be as low as possible. By knowing how the concentration varies through the depth profile the degassing can be reduced by elevating the water withdrawal level above the point of the highest measured concentrations. However this in turn gives less pressure on the turbines and less energy production, and a cost-benefit analysis would be needed. For reservoirs other than hydropower ones as CDU drinking water reservoir this is a more straightforward recommendation. Since the reservoirs emit the highest CH₄ emissions from young sediment there is a way to reduce the emissions by reducing the nutrient input for the first years. By implementing a reservoir management strategy that reduces autochthonous primary production a decrease of CH₄ emissions to the atmosphere could be achieved (Isidorova et al., 2019). Since there is a hydropower boom in tropical areas there is now a risk of escalating the CH₄ concentrations to the atmosphere. By striving to optimize nutrient application efficiency and especially nutrient removal from wastewater this effect can be mitigated and hopefully reduce the addition of anthropogenic CH₄ which increase the atmospheric radioactive force. The model strategy that is proposed in this report could be used in the future as an more accessible way of predicting the methane emissions from the degassing process of hydropower reservoirs. Using the model has also the advantages of being able to predict future emissions can also be done by adding suitable climate factors to the meteorology data.

6 CONCLUSION

This study has shown that by analysing water samples from the entire water profile before the water intake in the drinking water reservoir Chapéu D'Uvas the CH₄ emission from the degassing process was estimated at 1.1 % of the total daily GHG emissions from the entire reservoir. The method of sampling deep-water CH₄ concentrations using the newly developed deep-water sampler worked well and can be replicated and used for other reservoirs. By comparing the results of the emissions from Chapéu D'Uvas with values from the degassing emissions of hydropower reservoirs found in the literature the degassing processes from the drinking water reservoir Chapéu D'Uvas were low.

There is a possibility to model the CH₄ concentrations in water profiles from reservoir using measurements of temperature profiles from the reservoir and empirical models of oxygen demand and CH₄ production. The first step of modeling a consistent daily water temperature profiles was done in this study and the results from the model can be used to continue this process by adding the oxygen consumption rate and the CH₄ formation rate as functions of temperature and total nitrogen. The results for the calibrated GOTM model were able to capture the broad seasonal changes of the waters temperature, stratification and mixing. The modeled profiles gave a good estimation of the water temperature for the deeper water levels for months when the water was clearly stratified but for months when the water was more mixed it predicted water profiles with lower model fit. The predictions from the model can be used to continue the implementation of the next steps for the CH₄ concentration model proposed in this report.

REFERENCES

- Abril, G., Guérin, F., Richard, S., Delmas, R., Galy-Lacaux, C., Gosse, P., Tremblay, A., Varfalvy, L., Santos, M. A. D. and Matvienko, B. (2005), 'Carbon dioxide and methane emissions and the carbon budget of a 10-year old tropical reservoir (petit saut, french guiana)', *Global biogeochemical cycles* **19**(4), GB4007–n/a.
- Barros, N., Cole, J. J., Tranvik, L. J., Prairie, Y. T., Bastviken, D., Huszar, V. L. M., del Giorgio, P. and Roland, F. (2011), 'Carbon emission from hydroelectric reservoirs linked to reservoir age and latitude', *Nature geoscience* **4**(9), 593–596.
- Burchard, H. (2002), *Applied turbulence modelling in marine waters*, Vol. 100, Springer, New York;Berlin;.
- Cardoso, S. J., Enrich-Prast, A., Pace, M. L. and Roland, F. (2014), 'Do models of organic carbon mineralization extrapolate to warmer tropical sediments?', *Limnology and oceanography* **59**(1), 48–54.
- Church, J., Clark, P., Cazenave, A., Gregory, J., Jevrejeva, S., Levermann, A., Merrifield, M., Milne, G., Nerem, R., Nunn, P., Payne, A., Pfeffer, W., Stammer, D. and Alakkat, U. (2013), 'Climate change 2013: The physical science basis. contribution of working group i to the fifth assessment report of the intergovernmental panel on climate change', *Sea Level Change* pp. 1138–1191.
- Cole, J. J. and Caraco, N. F. (1998), 'Atmospheric exchange of carbon dioxide in a low-wind oligotrophic lake measured by the addition of sf₆', *Limnology and oceanography* **43**(4), 647–656.
- Cole, J. J., Prairie, Y. T., Caraco, N. F., McDowell, W. H., Tranvik, L. J., Striegl, R. G., Duarte, C. M., Kortelainen, P., Downing, J. A., Middelburg, J. J. and Melack, J. (2007), 'Plumbing the global carbon cycle: Integrating inland waters into the terrestrial carbon budget', *Ecosystems (New York)* **10**(1), 172–185.
- dos Santos, M. A., Damázio, J. M., Rogério, J. P., Amorim, M. A., Medeiros, A. M., Abreu, J. L. S., Maceira, M. E. P., Melo, A. C. and Rosa, L. P. (2017), 'Estimates of ghg emissions by hydroelectric reservoirs: The brazilian case', *Energy (Oxford)* **133**, 99–107.
- Duchemin, E., Lucotte, M., Canuel, R. and Chamberland, A. (1995), 'Production of the greenhouse gases ch₄ and co₂ by hydroelectric reservoirs of the boreal region', *Global biogeochemical cycles* **9**(4), 529–540.
- Earth, G. (2020), 'Brazil'.
URL: <http://www.earth.google.com>
- Fenchel, T., King, G. and Blackburn, T. H. (2012), *Bacterial biogeochemistry: the ecophysiology of mineral cycling*, third edn, Elsevier/AP, London.
- Grasset, C., Mendonça, R., Villamor Saucedo, G., Bastviken, D., Roland, F. and Sobek, S. (2018), 'Large but variable methane production in anoxic freshwater sediment upon addition of allochthonous and autochthonous organic matter', *Limnology and oceanography* **63**(4), 1488–1501.
- Gudasz, C., Bastviken, D., Steger, K., Premke, K., Sobek, S. and Tranvik, L. J. (2010), 'Erratum: Temperature-controlled organic carbon mineralization in lake sediments', *Nature (London)* **466**(7310), 1134–1134.
- Guérin, F. and Abril, G. (2007), 'Significance of pelagic aerobic methane oxidation in the methane and carbon budget of a tropical reservoir', *Journal of Geophysical Research: Biogeosciences* **112**(G3), G03006–n/a.
- Guérin, F., Abril, G., Richard, S., Burban, B., Reynouard, C., Seyler, P. and Delmas, R. (2006), 'Methane and carbon dioxide emissions from tropical reservoirs: Significance of downstream rivers', *Geophysical research letters* **33**(21).
- Guérin, F., Abril, G., Serça, D., Delon, C., Richard, S., Delmas, R., Tremblay, A. and Varfalvy, L. (2007), 'Gas transfer velocities of co₂ and ch₄ in a tropical reservoir and its river downstream', *Journal of marine systems* **66**(1-4), 161–172.
- Hertwich, E. G. (2013), 'Addressing biogenic greenhouse gas emissions from hydropower in lca', *Environmental science technology* **47**(17), 9604–9611.

- Hoffert, M. I., Caldeira, K., Jain, A. K., Haites, E. F., Harvey, L. D. D., Potter, S. D., Schlesinger, M. E., Schneider, S. H., Watts, R. G., Wigley, T. M. L. and Wuebbles, D. J. (1998), 'Energy implications of future stabilization of atmospheric co₂ content', *Nature (London)* **395**(6705), 881–884.
- Isidorova, A., Grasset, C., Mendonça, R. and Sobek, S. (2019), 'Methane formation in tropical reservoirs predicted from sediment age and nitrogen', *Scientific reports* **9**(1), 11017–11017.
- Jähne, B., Münnich, K. O., Börsinger, R., Dutzi, A., Huber, W. and Libner, P. (1987), 'On the parameters influencing air-water gas exchange', *Journal of Geophysical Research* **92**(C2), 1937–1949.
- Kelly, C. A., Rudd, J. W. M., Bodaly, R. A., Roulet, N. P., St.Louis, V. L., Heyes, A., Moore, T. R., Schiff, S., Aravena, R., Scott, K. J., Dyck, B., Harris, R., Warner, B. and Edwards, G. (1997), 'Increases in fluxes of greenhouse gases and methyl mercury following flooding of an experimental reservoir', *Environmental science technology* **31**(5), 1334–1344.
- Kemenes, A., Forsberg, B. R. and Melack, J. M. (2011), 'Co₂ emissions from a tropical hydroelectric reservoir (balbina, brazil)', *Journal of Geophysical Research: Biogeosciences* **116**(G3), n/a.
- Kemenes, A., Forsberg, B. R. and Melack, J. M. (2016), 'Downstream emissions of ch₄ and co₂ from hydroelectric reservoirs (tucuruí, samuel, and curuá-una) in the amazon basin', *Inland waters (Print)* **6**(3), 295–302.
- Kumar A, Schei T, A. A. (2011), 'Hydropower. in: Ipcc special report on renewable energy sources and climate change mitigation'.
- Li, S., Zhang, Q., Bush, R. T. and Sullivan, L. A. (2015), 'Methane and co₂ emissions from china's hydroelectric reservoirs: a new quantitative synthesis', *Environmental science and pollution research international* **22**(7), 5325–5339.
- Likens, G. E. (2009), *Encyclopedia of Inland Waters*, Academic Press [Imprint], San Diego.
- Linkhorst, A. (2019), *Greenhouse gas emission from tropical reservoirs: Spatial and temporal dynamics*, Vol. 1859.
- Moras, S., Ayala, A. I. and Pierson, D. C. (2019), 'Historical modelling of changes in lake erken thermal conditions', *Hydrology and earth system sciences* **23**(12).
- Paranaíba, J. R., Barros, N., Mendonça, R., Linkhorst, A., Isidorova, A., Roland, F., Almeida, R. M. and Sobek, S. (2018), 'Spatially resolved measurements of co₂ and ch₄ concentration and gas-exchange velocity highly influence carbon-emission estimates of reservoirs', *Environmental science technology* **52**(2), 607–615.
- Reeburgh, W. S., Whalen, S. C. and Alperin, M. J. (1993), 'The role of methylophony in the global methane budget, in microbial growth on c₁ compounds'.
- Rodriguez, M. and Casper, P. (2018), 'Greenhouse gas emissions from a semi-arid tropical reservoir in northeastern brazil', *Regional environmental change* **18**(7), 1901–1912.
- Rudd, J. W. M., Harris, R., Kelly, C. A. and Hecky, R. E. (1993), 'Are hydroelectric reservoirs significant sources of greenhouse gases?', *Ambio* **22**(4), 246–248.
- Rzóska, J. (1981), 'Baxter, r. m., and p. glaupe. 1980. environmental effects of dams and impoundments in canada: Experience and prospects. can. bull. fish. aquat. sci. 205. dept. fish. oceans, ottawa, vi + 34 p. in canada c 2.50; elsewhere c 3.00', *Limnology and oceanography* **26**(5), 998–999.
- Scherer, L. and Pfister, S. (2016), 'Hydropower's biogenic carbon footprint', *PloS one* **11**(9), e0161947–e0161947.
- Smith, S. J., Edmonds, J., Hartin, C. A., Mandra, A. and Calvin, K. (2015), 'Near-term acceleration in the rate of temperature change', *Nature climate change* **5**(4), 333–336.

- Stepanenko, V., Mammarella, I., Ojala, A., Miettinen, H., Lykosov, V. and Vesala, T. (2016), 'Lake 2.0: a model for temperature, methane, carbon dioxide and oxygen dynamics in lakes', *Geoscientific model development* **9**(5), 1977–2006.
- Torbert, H., Rogers, H., Prior, S., Schlesinger, W. and Brett Runion, G. (1997), 'Effects of elevated atmospheric CO₂ in agro-ecosystems on soil carbon storage', *Global change biology* **3**(6), 513–521.
- Tranvik, L. J., Downing, J. A., Cotner, J. B., Loiselle, S. A., Striegl, R. G., Ballatore, T. J., Dillon, P., Finlay, K., Fortino, K., Knoll, L. B., Kortelainen, P. L., Kutser, T., Larsen, S., Laurion, I., Leech, D. M., McCallister, S. L., McKnight, D. M., Melack, J. M., Overholt, E., Porter, J. A., Prairie, Y., Renwick, W. H., Roland, F., Sherman, B. S., Schindler, D. W., Sobek, S., Tremblay, A., Vanni, M. J., Verschoor, A. M., von Wachenfeldt, E. and Weyhenmeyer, G. A. (2009), 'Lakes and reservoirs as regulators of carbon cycling and climate', *Limnology and oceanography* **54**(6part2), 2298–2314.
- Van't Hoff, J. H. V. (1884), *Etudes de dynamique chimique*, Frederik Muller.
- West, W. E., Coloso, J. J. and Jones, S. E. (2012), 'Effects of algal and terrestrial carbon on methane production rates and methanogen community structure in a temperate lake sediment', *Freshwater biology* **57**(5), 949–955.
- Wilkinson, J., Maeck, A., Alshboul, Z. and Lorke, A. (2015), 'Continuous seasonal river ebullition measurements linked to sediment methane formation', *Environmental science technology* **49**(22), 13121–13129.
- Winton, R. S., Calamita, E. and Wehrli, B. (2019), 'Reviews and syntheses: Dams, water quality and tropical reservoir stratification', *Biogeosciences* **16**(8), 1657–1671.
- Yvon-Durocher, G., Allen, A. P., Bastviken, D., Conrad, R., Gudas, C., St-Pierre, A., Thanh-Duc, N. and del Giorgio, P. A. (2014), 'Methane fluxes show consistent temperature dependence across microbial to ecosystem scales', *Nature (London)* **507**(7493), 488–491.
- Zarfl, C., Lumsdon, A. E., Berlekamp, J., Tydecks, L. and Tockner, K. (2015), 'A global boom in hydropower dam construction', *Aquatic sciences* **77**(1), 161–170.

APPENDICES

Table 1. Concentration of CH_4 in (g/m^3) and (nM) for waterprofile in front of intake for CDU

Lable	Depth (m)	CH4 Cw (g/m^3)	CH4 Cw (nM)
S121	0	0.006453286	403.330395
S81	0	0.005378071	336.129417
S14	5	0.000919527	57.470446
D51	5	0.000817906	51.119143
I10	5	0.000944948	59.059241
D44	5	0.000615187	38.449199
S64	10	0.000434327	27.145446
S23	10	0.000415528	25.970506
D61	10	0.000393278	24.579885
S1	10	0.000532079	33.254932
F119	15	0.000418087	26.130447
S58	15	0.00027572	17.232503
C6	15	0.00032884	20.552490
S95	15	0.000342404	21.400242
D6	20	0.002191178	136.948655
S94	20	0.002307762	144.235111
I05	20	0.00406354	253.971249
D31	20	0.002266287	141.642955
D18	25	0.151919515	9494.969698
S13	25	0.139914925	8744.682796
S82	25	0.109420152	6838.759486
D26	25	0.121644233	7602.764552
S78	30	0.006518011	407.375706
S87	30	0.002904673	181.542063
D46	30	0.002567314	160.457116
S18	30	0.002710948	169.434252
I09	35	0.008322011	520.125692
D4	35	0.009309753	581.859578
S51	35	0.00891702	557.313774
D29	35	0.012224755	764.047194

From $CH_{4,mol}$ to $CH_{4,ppm}$

$$\frac{CH_{4,mol}}{\frac{(airpressure_{bar})}{(V_{injected}(ml))}} * 8.314 * T(K) = CH_{4,ppm} \quad (9)$$

To $CH_{4,water}$ (mol)

$$CH_4 * 10^{-6} * (mol/L * atm * V_{waterequilibrated}(L)) * 10^9 = CH_{4w,ater}(mol) \quad (10)$$

To $CH_{4,gas}$ (mol)

$$\frac{(CH_{4,ppm} * 10^{-6}) * V_{gaseq}(ml) * atmpressure}{(1000 * 0.082057 * T_{eq}(K))} * 10^9 = CH_{4,gas}(mol) \quad (11)$$

To $CH_{4,air}$ (mol)

$$\frac{V_{gasequilibrated}(L) * CH_{4background,atm} * atm}{((0.082057 * T_{equilibrated}(K)))} * 10^9 = CH_{4,air} \quad (12)$$

To $CH_{4,water}$ g m³

$$\frac{CH_{4,water} + CH_{4,air} + CH_{4,gas}}{V_{collectedwater}} * 10^{-6} * 16 = CH_{4,water} \quad (13)$$

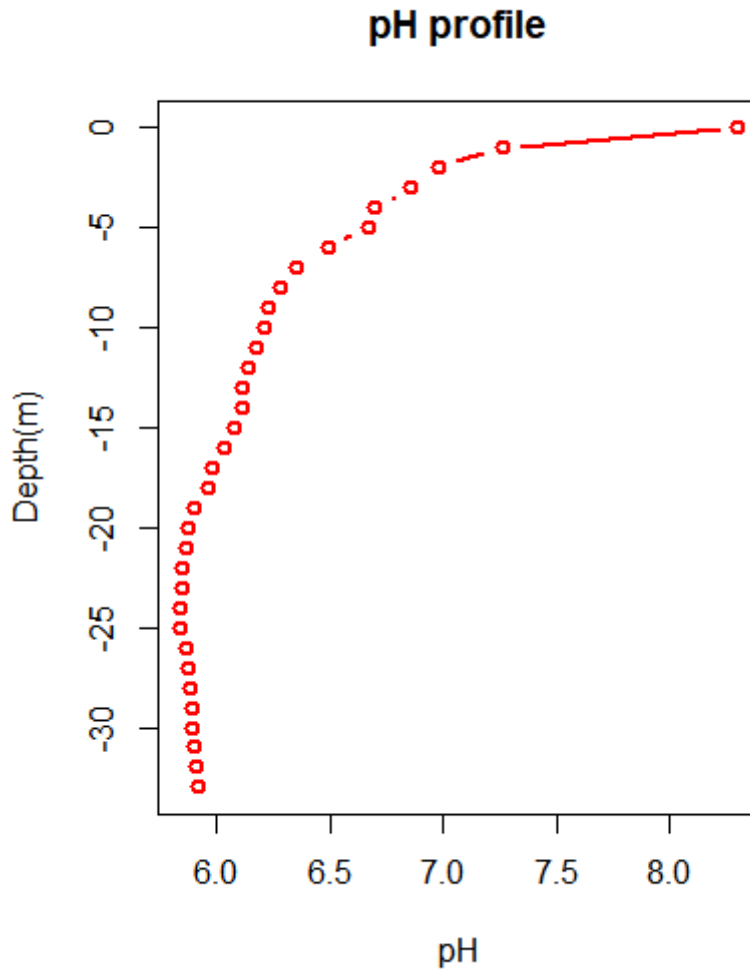


Figure A1. pH profile from CDU.

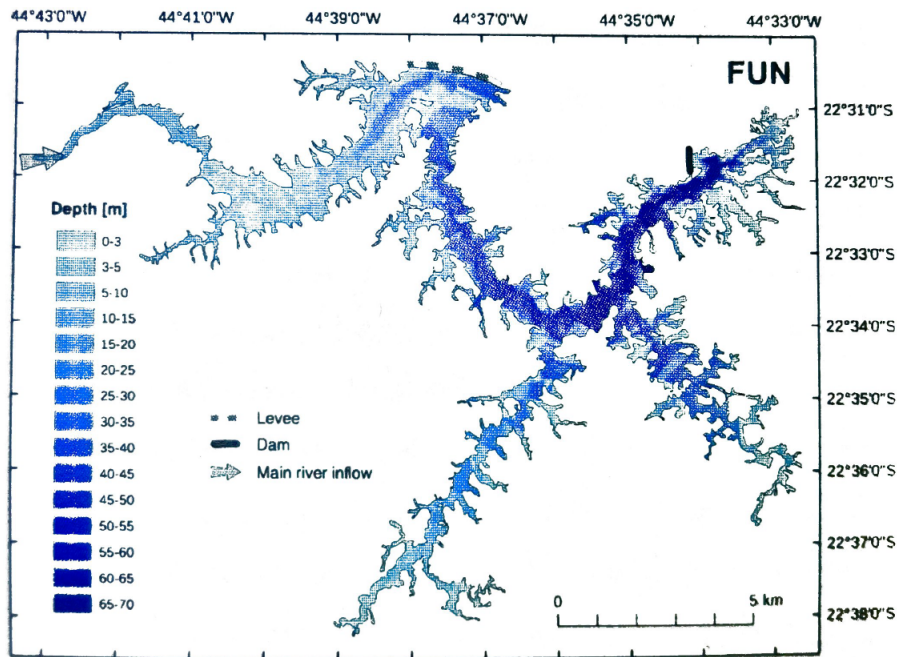


Figure A2. Bathymetric map of Funil(FUN) reservoir from October 2016 from, map made of Annika Linkhorst (2019)

Table 2. Hypsograph of FUN

Depth	Water volume m ³
0	35000000
2	32000000
4	31000000
6	30000000
8	29500000
10	29000000
12	25810000
14	18067000
16	12646900
18	8852830
20	6196981
22	4337886
24	3036520
26	2125564
28	1487895
30	1041526
32	729068
34	510348
36	357243
38	250070
40	175049
42	122534
44	85774
46	60041
48	42029
50	29420
52	20594
54	14416
56	10091
58	7063
60	4944

R.studio script used to calculate the CH₄ concentration.

```
### THIS SCRIPT IS FOR THE MICROPORTABLE GGA ###

#This reads file in .csv format EXACTLY in the form you downloaded
  ↪ from the Los Gatos

CH4_x<- read.csv(file.choose(), header=F) #load .csv data, choose .txt file
  ↪ from the los gatos
head(CH4_x) #check what you loaded, it is displayed in the R console

#Run next lines to transform the file loaded
CH4=as.numeric(as.character(CH4_x[,9]))
len <- length(na.omit(CH4))+2
CH4 <- rnorm(0)
CH4 <- as.numeric(as.character(CH4_x[3:len,9]))
all <- CH4_x[1:len,] #extract time data only
k <- as.character(all[,1]) #transform them to character
t <- unlist(strsplit(k, "_"))
p <- rnorm(0)
l <- 9
o <- 1
for (i in 1:len) {
  p[o]=t[l]
  l=l+2
  o=o+1
}
j <- unlist(strsplit(p, ":"))
j <- as.numeric(j)
o=1
time=rnorm(0)
for (i in 1:(length(j)/3)) {
time[i]=(j[o]-j[l])*60+j[o+1]+j[o+2]/60
o=o+3 }
ifelse (length(time)==length(CH4),"can_continue","something_went_wrong,_try
  ↪ _again")

#Look in the R console, if it allows you to continue

#Before running your peaks run the function below ("area") to
  ↪ activate it (just once per session)

#Open los gatos file with excel and look in which line your peak
  ↪ starts and ends, you dont need to change anything in the los
  ↪ gatos file

#Copy the result in your excel file

a <- 8088 # enter line number when the peak starts
b <- 8108 # enter line number when the peak ends
int(time[(a-2):(b-2)]*60*10, CH4[(a-2):(b-2)])
plot(time[(a-2):(b-2)],CH4[(a-2):(b-2)],type="o", xlab="time,_min", ylab="
```

```

    ↪ CH4, _ppm") #plot the peak
quartz(height=5,width=5)
plot(time*60,CH4, type="l") #plot whole file

#Run this function once
  int <- function(x,y) #function for integration of the peak
  {
area <- 0
c <- length(x[x>0])
  for (i in 2:c) {
    if (y[i]-y[i-1]>=0 & x[i]>0)
area <- (x[i]-x[i-1])*y[i-1] + ((x[i]-x[i-1])*(y[i]-y[i-1]))/2+area
    if (y[i]-y[i-1]<0 & x[i]>0)
area <- (x[i]-x[i-1])*y[i] + ((x[i]-x[i-1])*(y[i-1]-y[i]))/2+area
  }
if (y[c]>=y[1])
area <- area-y[1]*(x[c]-x[1])-(y[c]-y[1])*(x[c]-x[1])/2

if (y[c]<y[1])
area <- area-y[c]*(x[c]-x[1])-(y[1]-y[c])*(x[c]-x[1])/2

mol <- 0

if (area<=1000)
mol=area*0.0000000000351207542455684+0.000000000436628595995149
if (area<=1000000 & area>1000)
mol=area*0.0000000000399819686171373-0.0000000243143691910771
if (area>1000000)
mol=area*0.0000000000739629703779142-0.0000116830441182922
return(paste ("area=", area, "_mol=", mol))
  }

```